Tracking the evolution of magmas from heterogeneous mantle sources to eruption

A. Mallik[1]†, S. Lambart[2]†, and E.J. Chin[3]†

[1]Department of Geosciences, University of Rhode Island.

[2]Department of Geology and Geophysics, University of Utah.

[3]Scripps Institution of Oceanography, University of California, San Diego.

Corresponding author: Ananya Mallik (ananya_mallik@uri.edu)

†Equally contributing authors

Key Points:

- Effects of source heterogeneity and intracrustal differentiation on magma chemistry is explored

- Discussion is based on experimental studies and compositions of about 60,000 natural volcanic rocks, melt inclusions and cumulates

- Magmatism in mid-ocean ridges, ocean islands and arcs are considered.

Abstract

This contribution reviews the effects of source heterogeneities, melt-rock reactions and intracrustal differentiation on magma chemistry across mid-ocean ridges, intraplate settings and subduction zones using experimental studies and natural data. We compare melting behaviors of pyroxenites and peridotites and their relative contributions to magmas as functions of composition, mantle potential temperatures and lithospheric thickness. We also discuss the fate of chemically distinct melts derived from heterogeneities as they travel through a peridotitic mantle. Using nearly 60,000 natural major element compositions of volcanic rocks, melt inclusions, and crystalline cumulates, we assess broad petrogenetic trends in as large of a global dataset as possible. Consistent with previous studies, major element chemistry of mid-ocean ridge basalts (MORBs) and their cumulates favor a first-order control of intracrustal crystal-liquid segregation, while trace element studies emphasize the role of melt-rock reactions, highlighting the decoupling between the two. Ocean island basalts (OIB) show a larger compositional variability than MORB, partly attributed to large variations of pyroxenite proportions in the mantle source. However, the estimated proportions vary considerably with heterogeneity composition, melting model and thermal structure of the mantle. For arcs, we highlight current views on the role of the downgoing slab into the source of primary arc magmas, and the role of the overriding lithosphere as a magmatic chemical filter and as the repository of voluminous arc cumulates. Our approach of simultaneously looking at a large database of volcanic + deep crustal rocks across diverse tectonic settings underscores the challenge of deciphering the source signal versus intracrustal/lithospheric processes.

Plain Language Summary

Volcanic rocks on Earth share a common history – melting in the mantle tens to hundreds of kilometers deep, traveling through the mantle to the crust, and cooling and partial crystallizing in the crust, before finally reaching the surface – and yet, they show an incredible compositional variability. What creates such variability? In this chapter, we discuss the potential causes by looking at the role of the heterogeneities in the mantle and the fate of the magmas along their journey to the surface through the mantle and the crust. The discussion is based on experimental studies and natural compositions of about 60,000 volcanic rocks, melt inclusions (small pools of magma trapped inside the minerals) and cumulates (products of the crystallization of the magmas) from three main geological settings: divergent plate boundaries (mid-ocean ridges), intra tectonic plates (oceanic islands) and convergent plate boundaries (subduction zones).

1 Introduction

Magmatism on Earth takes place at three main different tectonic settings: mid-ocean ridges, intraplate settings including ocean islands, and arc magmatism in subduction zones. The upper mantle, mostly composed of peridotites, is the main source of magma on Earth. However, geophysical, geochemical and field observations demonstrate that the mantle is heterogeneous. Many studies have proposed that crustal lithologies introduced in the Earth's mantle by subduction, including sediments and oceanic crust contribute significantly as heterogeneities to the generation of mantle-derived magmas (e.g. Chase, 1981; Helffrich and Wood, 2001; Hirschmann and Stolper, 1996; Hofmann, 1997; Hofmann and White, 1982; Jackson et al., 2007; Lambart, 2017; Lambart et al., 2009, 2016; Mallik and Dasgupta, 2012; Salters and Dick, 2002; Schiano et al., 1997; Sobolev et al., 2005, 2007). The contribution of a lithology during magma genesis is controlled by four main parameters: (1) the fraction of the lithology in the mantle, (2) its solidus temperature, (3) its melt productivity, and (4) the mantle regime (potential temperature and thickness of the lithosphere). In this chapter, we discuss the current state of understanding of how these parameters affect the contribution of heterogeneities in magma generation in the Earth's upper mantle across the three tectonic settings. We also review perspectives on magmatic differentiation, since intracrustal differentiation is the "last mile" of a primary magma's journey from its origin as a partial melt of the mantle to its point of eruption. Disentangling the contributions from differentiation vs. source heterogeneity are therefore non-trivial. To these ends, we review results from experimental studies simulating partial melting under a variety of upper mantle conditions and compositions. Then we compare experimental results with a compilation of nearly 60,000 compositions of natural volcanic rocks, melt inclusions, and plutonic cumulate rocks from ridges, intraplate settings, and volcanic arcs.

2 Partial melting of a heterogeneous mantle

2.1 Contribution of mantle lithologies to magma genesis

For the purpose of this section, we use the term "pyroxenite" to refer to mafic and ultramafic-rich plutonic rocks that lack sufficient olivine (40%) to be classified as peridotites (Le Maitre et al., 2005). Based on their abundance in orogenic massifs, it is generally assumed that the Earth's upper mantle contains 2 to 5% of pyroxenites (e.g., Bodinier and Godard, 2003). Magma compositions suggest that the mantle source can be significantly enriched locally (e.g., Sobolev et al., 2005) or even be exclusively composed of pyroxenites (e.g., Zhang et al., 2018). Compositions of the lithologies control their solidus temperatures and melt productivities (Hirschmann, 2000; Lambart et al., 2016; Pickering-Witter and Johnston, 2000), while thermal structure of the mantle and the crust control the melt fluxes and initial and final pressures of melting (Langmuir et al., 1992; Sleep, 1990; Tatsumi et al., 1983). The influence of composition on the solidus temperatures of mantle lithologies has been the subject of several experimental and theoretical studies (Hirschmann, 2000; Kogiso and Hirschmann, 2006; Kogiso et al., 2004; Lambart et al., 2016). These studies demonstrate that, at a given pressure, the solidus temperatures of anhydrous and CO_2-free lithologies are mostly influenced by the bulk alkali content **(Fig. 1)** and Mg-number (Mg#=molar MgO/[molar MgO+molar FeO^T] of the rock.
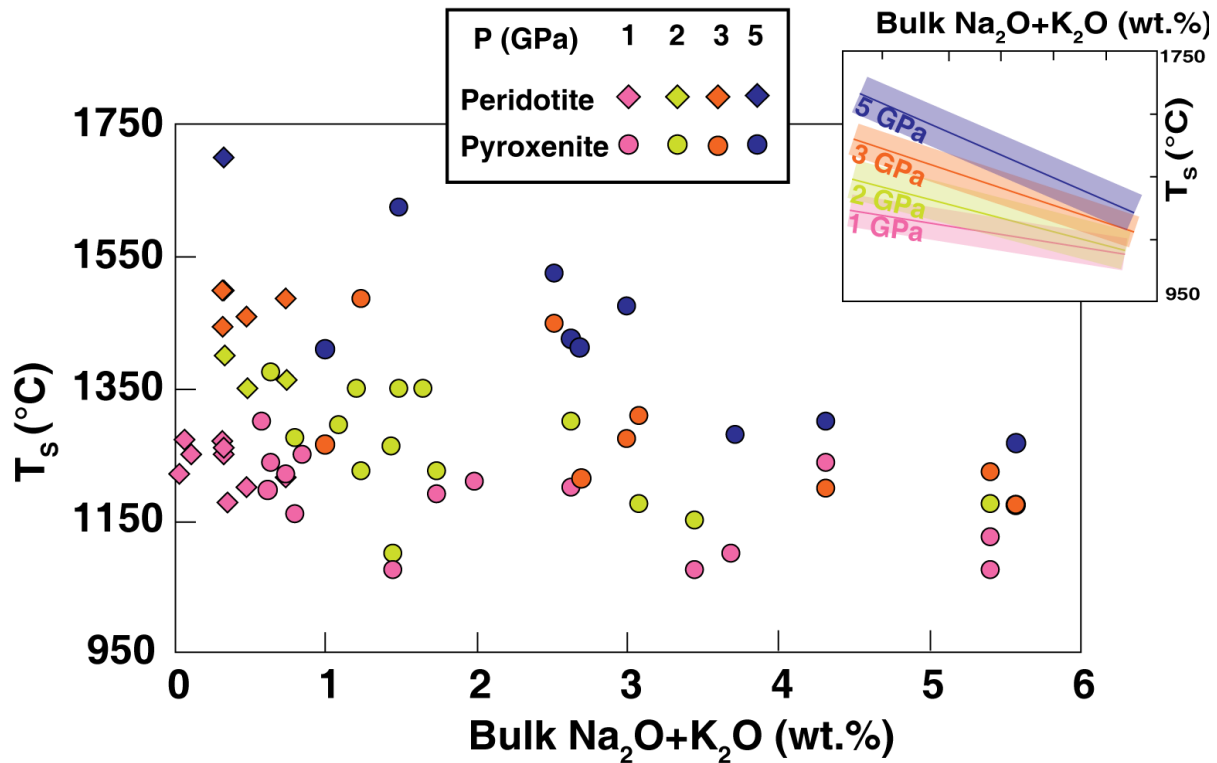
Figure 1. Pyroxenite and peridotite solidus temperatures determined experimentally as a function of the bulk alkali content for pressures between 1 and 5 GPa. The inset shows the linear regressions for each pressure and the corresponding error envelopes (1σ). References: Adam et al., 1992; Baker and Stolper, 1994; Borghini et al., 2017; Hirose and Kushiro, 1993; Hirschmann et al., 2003; Ito and Kennedy, 1974; Kogiso et al., 1998; Kogiso and Hirschmann, 2001,2006; Kogiso et al., 2003; Kornprobst, 1970; Kushiro, 1996; Lambart et al., 2009, 2012; Pertermann and Hirschmann, 2003a; Pickering-Witter and Johnston, 2000; Rosenthal et al., 2014, 2018; Schwab and Johnston, 2001; Spandler et al., 2008, 2010; Thompson, 1974, 1975; Tsuruta and Takahashi, 1998; Tuff et al., 2005; Walter, 1998; Wasylenki et al., 2003; Yasuda et al., 1994

Fewer studies, however, discuss the controls on melt productivity. Melt productivities of mantle lithologies tend to increase with the contribution of clinopyroxene (cpx; Lambart et al., 2013; Pertermann and Hirschmann, 2003a; Pickering-Witter and Johnston, 2000; Spandler et al., 2008) and feldspar (Falloon et al., 2008; Lambart et al., 2009; Spandler et al., 2008) in the melting reaction. On the contrary, the presence of other accessory phases like rutile, quartz, spinel or olivine results in low melt productivities, explained by a low thermodynamic variance of the system (Pertermann and Hirschmann, 2003a). **Figure 2** compares experimental melt fractions as a function of temperature at 1 and 3 GPa for various pyroxenite and peridotite compositions. The higher solidus temperature difference between pyroxenites and peridotites at 3 GPa than at 1 GPa partly reflects sampling bias (most experiments at 3 GPa were performed on alkali-richer and Mg-poorer lithologies than experiments performed at 1 GPa), but is also consistent with the parameterization of Lambart et al. (2016) that shows that the solidus temperature variation in pyroxenites significantly decreases with pressure.
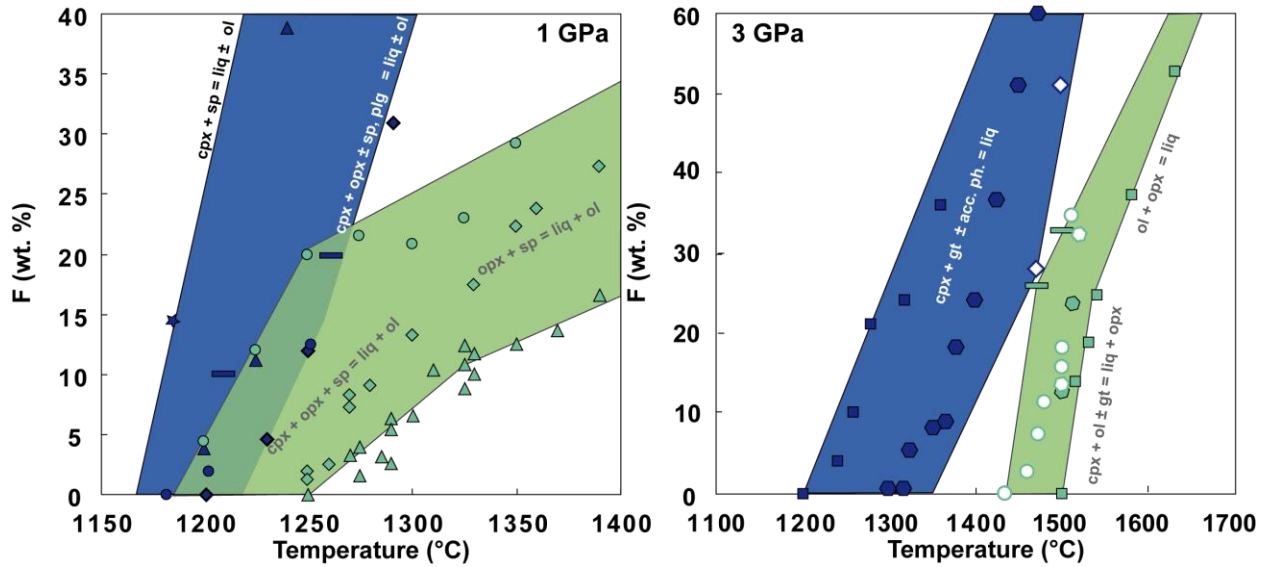
Figure 2. Experimental melt fractions as functions of temperature for pyroxenites (blue: M7-16, star; M5-40, triangles; M5-103, diamonds; GV10, rectangles; Ito and Kennedy's eclogite, circles; GA2, squares; G2, hexagons; B-ECL1, open diamonds)) and peridotites (green: PHN-1611, circles; MM3, diamonds; DDMM, triangles; KR4003, square; KLB-1, open circles; HK66, rectangles; KG2, hexagons; KG1,open hexagons) at 1 and 3 GPa. The blue and green fields show the envelopes of melt fractions for pyroxenites and peridotites, respectively. References: Baker and Stolper (1994), Baker et al., (1995), Borghini et al. (2017), Hirose and Kushiro (1993), Hirschmann et al. (1998), Ito and Kennedy (1974), Kogiso and Hirschmann (2006), Kogiso et al. (1998), Kushiro (1996), Lambart et al. (2009), Pertermann and Hirschmann (2003a), Spandler et al. (2008), Walter (1998), Wasylenki et al. (2003).

Peridotites are marked by a decrease in melt productivity when cpx disappears from the experimental assemblage. However, the productivities of pyroxenites and peridotites are scattered but largely overlap before cpx disappearance. Hence, the cpx disappearance in the mineralogical assemblage is the main parameter influencing the large difference in melt productivity between peridotites and pyroxenites.
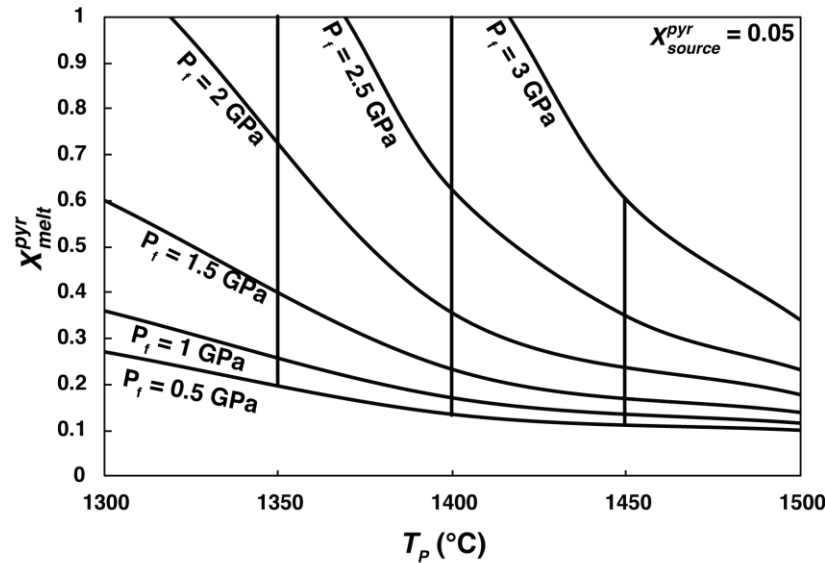
Figure 3. Effect of potential temperature (T_P) and the final pressure of melting (P_f) on the contribution of pyroxenite G2 (Pertermann and Hirschmann, 2003a) in the aggregated magma $X_{melt}^{pyr} = (X_{source}^{pyr} \times F_f^{pyr})/(X_{source}^{pyr} \times F_f^{pyr} + (1 - X_{source}^{pyr}) \times F_f^{per})$, assuming $X_{source}^{pyr} = 0.05$ and calculated with Melt-PX (Lambart et al., 2016).

Finally, the thermal structure of the mantle and the crust mostly controls the potential temperature (T_P) and the thickness of the lithosphere (considered as the final pressure of melting; e.g., Dasgupta et al., 2010). Decreasing T_P or increasing the thickness of the lithosphere both result in an increase of the low-solidus component contribution (usually, the pyroxenite) in the melt by decreasing the relative height of the melting column where both lithologies are melting **(Fig. 3)** (Ellam, 1992; Humphreys and Niu, 2009; Niu et al., 2011; Sobolev et al., 2007)**.**

2.2 Peridotite vs. pyroxenite: experimental melt compositions

2.2.1. Major elements

Pyroxenites are usually separated into two groups: silica-excess (SE) and silica-deficient (SD) pyroxenites. The garnet–pyroxene thermal divide separating these two groups (defined by the Enstatite - Diopside - Alumina plane in the $CaO-MgO-Al_2O_3-SiO_2$ tetrahedron; O'Hara, 1976) controls the melting relations of pyroxenites at high pressure ($\geq$ 2 GPa; Kogiso et al., 2004) when cpx and garnet are both present in the mineralogical assemblage. Lambart et al. (2013) reviewed the melting phase relations of pyroxenites and showed that there is a large overlap of compositions between melt produced by the different mantle lithologies. As a rule, there is a progressive transition from the liquids derived from SE compositions to SD compositions to peridotites rather than a sharp compositional contrast. The extreme variability of the pyroxenite melts and the progressive transition between melts from different lithologies make finding good markers for the presence of pyroxenites in the source challenging. Yang and Zhou (2013) and Yang et al. (2016) suggested that the FC3MS ($FeO/CaO-3*MgO/SiO_2$, in wt.%) parameter can help with distinguishing between pyroxenite- and peridotite-derived melts. Their analysis demonstrates that the upper boundary of the FC3MS value for peridotite melts is 0.65, while melts derived from pyroxenites cover a much larger range (-0.9 to 1.7).

More recently, Yang et al. (2019) proposed two new parameters (FCMS and FCKANTMS) and showed that using log ratio-based chemical markers help in reducing the temperature and pressure effects on the compositional heterogeneity of melts. However, we note that none of these parameters can help to distinguish between peridotite-derived and pyroxenite-derived melts for compositions producing low parameter values (i.e, mostly SD pyroxenites).

2.2.2. First Row Transition elements.

First Row Transition Element (Sc, Ti, V, Cr, Mn, Fe, Co, Ni, Cu, Zn) concentrations in magmas have been recently suggested as good indicators of the mantle source mineralogy (e.g., Davis et al., 2013; Herzberg, 2011; Humayun et al., 2004; Le Roux et al., 2010, 2011; Prytulak and Elliott, 2007; Qin and Humayun, 2008; Sobolev et al., 2005, 2007). Le Roux et al. (2011) showed that during partial melting of the upper mantle, olivine and orthopyroxene do not significantly fractionate Mn and Fe from each other and melts from garnet-free peridotite are expected to have similar Mn/Fe ratios as the source. In contrast, clinopyroxene and garnet, the dominant minerals in pyroxenitic assemblages (Kogiso et al., 2004), show strong fractionations, such that melts of pyroxenites or eclogites would be expected to produce melts with low Mn/Fe compared to peridotite partial melts (Humayun et al., 2004). However, experiments by Le Roux and coworkers only explored peridotitic mineral compositions at a limited range of pressure (1.5-2 GPa), while partition coefficients can vary depending on the compositions of the minerals and

melts (e.g., Davis et al., 2013; Wang and Gaetani, 2008) as well as with pressure and temperature (P-T) conditions (e.g., Matzen et al., 2013, 2017a).
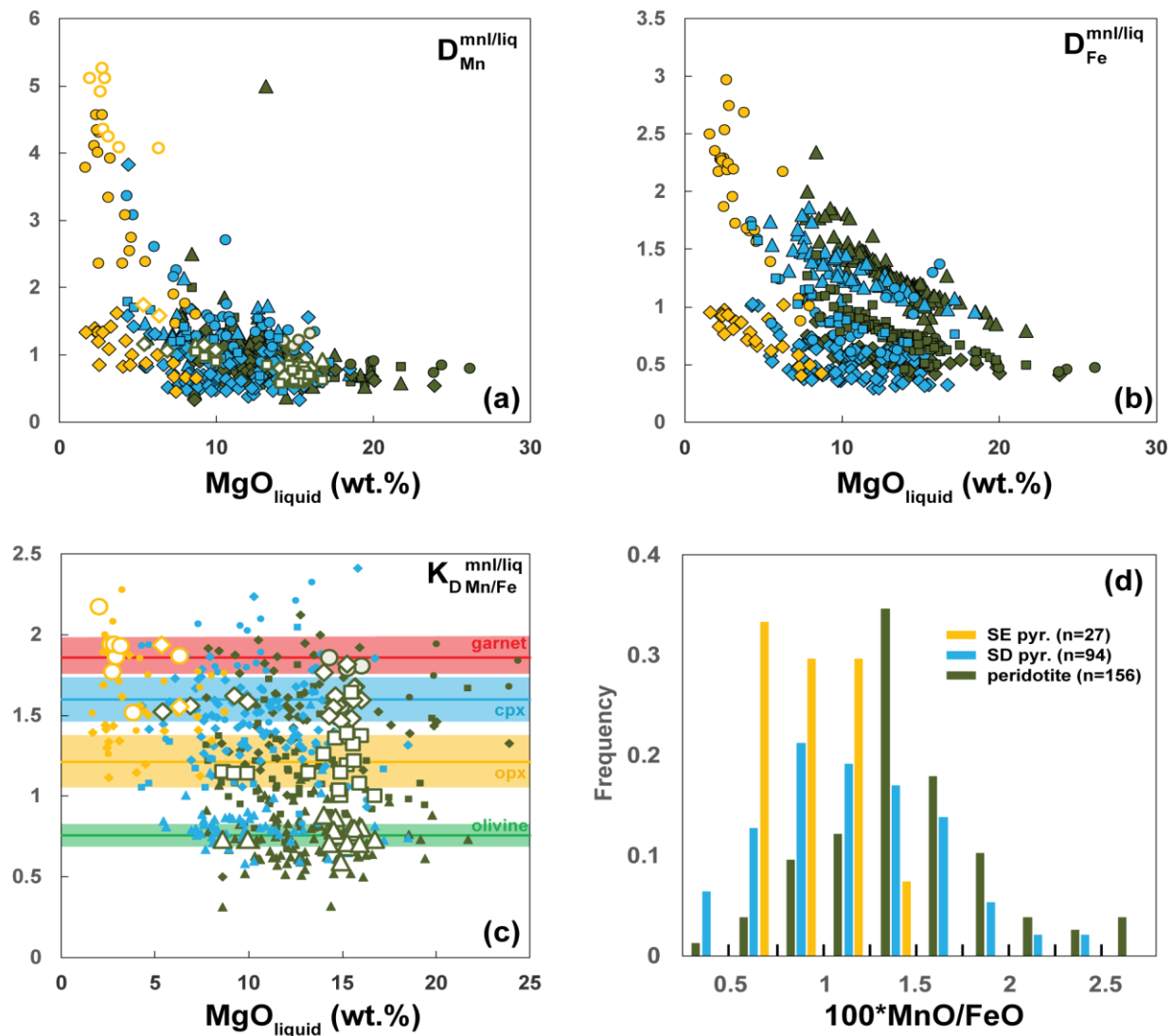
Figure 4. (a-b) Partition coefficient of Mn (a) and Fe (b) between minerals (garnet: circles; cpx: diamonds; opx: squares; olivine: triangles) as functions of the MgO content of the liquid for pyroxenites (SE: yellow; SD: blue) and peridotites (green). In (a), open symbols are higher accuracy analyses obtained by LA-ICP-MS or high current microprobe analyses (Davis et al., 2013; Le Roux et al., 2011; Pertermann et al., 2004). (c) Mn-Fe exchange partition coefficients (K_D) between minerals and melts. The colored lines show the average K_D calculated for each mineral using high accuracy measurements and the colored bands show the corresponding standard deviation. (d) Histogram showing the distributions of the 100*MnO/FeO ratios in experimental melts. References: Baker and Stolper (1994), Borghini et al. (2017), Davis et al. (2013), Falloon and Danyushevsky, (2000), Keshav et al., (2004), Kogiso and Hirschmann (2001, 2006), Kogiso et al. (2003), Lambart et al., (2009; compositions of the solid phases can be found at https://doi.org/10.6084/m9.figshare.9926885.v1), Lambart et al. (2013), Laporte et al. (2004), Le Roux et al. (2011), Pertermann and Hirschmann (2003b), Pickering-Witter and Johnston (2000), Pilet et al., (2008), Schwab and Johnston (2001), Walter (1998), Wasylenki et al. (2003), Yasuda et al. (1994), Yaxley and Sobolev, (2007).
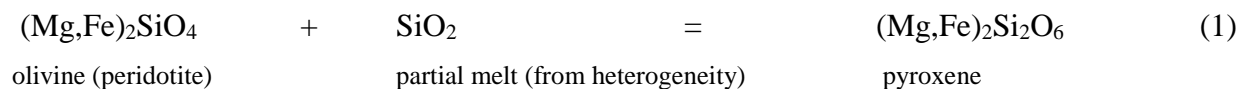
To take into account the potential effects of compositional and P-T variations, we plotted the partition coefficients between melt and mineral compositions using experiments reported in the literature on SE and SD pyroxenites and on peridotites. Partition coefficients for Fe and Mn
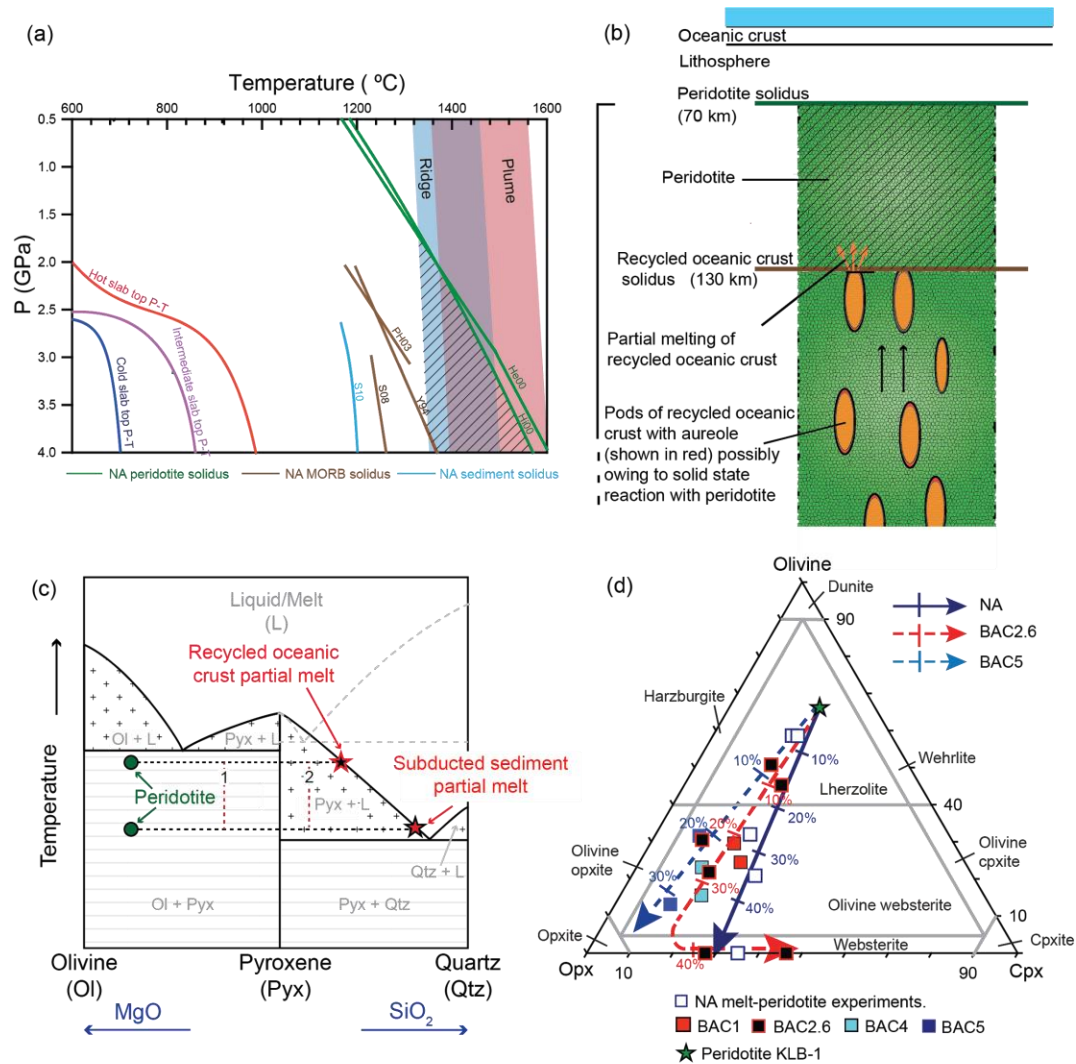
strongly depend on the MgO content of the melt **(Fig. 4a,b)**, but the Mn–Fe K_D are distinct for each mineral, and cpx-melt and garnet-melt Mn-Fe K_{DS} are distinctly higher than olivine-melt and opx-melt K_{DS} **(Fig. 4c)**. In addition to this, and in agreement with the results from Le Roux et al. (2011), Mn-Fe K_{DS} are independent of the composition. These results support the conclusions of Le Roux and coworkers: a mineral assemblage dominated by cpx and garnet will produce a melt with lower Mn/Fe ratio than a mineral assemblage dominated by olivine and orthopyroxene and, despite the large variability of bulk compositions that obscures this relationship, Mn/Fe ratio produced by pyroxenite-derived melts are generally lower than that in peridotite-derived melts **(Fig. 4d).**

3 Interactions between chemical heterogeneities and peridotite

Solidi of the nominally anhydrous subducted oceanic crust (e.g., Pertermann and Hirschmann, 2003a) and sediments (e.g., Spandler et al., 2010) are at lower temperatures than the solidus of nominally anhydrous peridotite-bearing ambient mantle **(Fig. 5a).** This implies that when the ambient peridotitic mantle carrying chemical heterogeneities upwells along an adiabat in the upper mantle **(Fig. 5b),** the heterogeneities reach their solidi temperatures deeper than the peridotite. Thus, between the solidi of heterogeneities and the peridotite (indicated by the dashed areas in **Figs. 5a** and **b**), the partial melt from heterogeneities would encounter subsolidus (unmelted) peridotite. The presence of volatiles such as H_2O and/or CO_2 in the heterogeneities further depress the solidi to lower temperatures (e.g. Dasgupta et al., 2004; Hammouda, 2003; Hermann and Spandler, 2008; Poli and Schmidt, 1995; Skora and Blundy, 2010; Yaxley and Brey, 2004) implying that the heterogeneities begin to partially melt even deeper in the upper mantle while the surrounding peridotite is still subsolidus. (An exception to this is under highly oxidized regions where CO_2 in peridotites may cause onset of carbonated silicate partial melting deeper than in the case of volatile-free peridotite (Dasgupta et al., 2013)).

The partial melts from these heterogeneities are not in equilibrium with subsolidus peridotites and will react with them (e.g., Kogiso et al., 1998; Mallik and Dasgupta, 2012; Yaxley and Green, 1998). Such a reactive melt-rock interaction can be illustrated by a simple binary phase diagram between olivine and quartz with double-eutectic at relevant pressures **(Fig. 5c).** (The readers are reminded that the binary phase diagram, while a useful tool to illustrate the first-order reactive crystallization process, does not capture the complexities imposed on the phase equilibria by a multi-component system that is a better analog to natural systems.) The siliceous partial melts from the heterogeneities lie on the liquidus surface of the pyroxene-quartz binary, while the peridotite lies below the solidus of the olivine-pyroxene binary. When the siliceous partial melts react with peridotite, the bulk composition of the melt-peridotite mixture is located between the partial melt and peridotite. Whether the bulk composition lies in the pyroxene-quartz binary or the olivine-pyroxene binary depends on the melt-rock proportion, where a higher proportion would place the bulk composition closer to the pyroxene-quartz binary. Thus, the interaction between the partial melt of the heterogeneities and peridotite would result in reactive crystallization, as observed in the phase diagram. The first order reaction that takes place in this context is as follows:

$$(Mg,Fe)_2SiO_4 \quad + \quad SiO_2 \quad = \quad (Mg,Fe)_2Si_2O_6 \quad\quad (1)$$

olivine (peridotite)   partial melt (from heterogeneity)   pyroxene

Figure 5. (a) Solidus of nominally anhydrous (NA) peridotite, recycled oceanic crust (MORB) and sediment plotted in pressure-temperature space. Also plotted for comparison are the range of adiabats from mid-ocean ridges to plume-settings with the lower end bracketed by mantle potential temperature of 1315 °C (McKenzie et al., 2005) and the higher end by 1550 °C (Herzberg et al., 2007), as well as hot, intermediate and cold subducted slab geotherms (Syracuse et al., 2010). The dashed area indicates P-T space where partial melt from recycled oceanic crust and sediments would react with the surrounding subsolidus peridotite. **(b)** Cartoon showing a slice of upwelling peridotitic mantle with pods of lithological heterogeneity (e.g. 5 wt.% recycled oceanic crust). NA recycled oceanic crust encounters its solidus at a depth ≈ 130 km, while the NA peridotite is still below the solidus. In the dashed area (the same as in panel a), partial melt derived from recycled oceanic crust undergoes reactive infiltration through the surrounding subsolidus peridotite. **(c)** Binary phase diagram between olivine and quartz (not to scale) with double eutectic, at 2.5 GPa (Chen and Presnall, 1975). Dashed gray lines in the pyroxene-quartz binary represent the solidus and liquidii in a pure MgO-SiO$_2$ system, solid lines represent solidus and liquidii with alkalis included. '1' indicates a bulk composition with low melt-rock ratio resulting in complete consumption of the melt and producing olivine-pyroxene residue. '2' indicates a bulk composition with high melt-rock ratio which produces a pyroxene residue by consuming olivine, and a residual melt that is less siliceous and more magnesian than the melt directly derived from chemical heterogeneities. **(d)** Streikeisen diagram for ultramafic rocks. The peridotite KLB-1 (Takahashi, 1986) is representative of a shallow upper mantle peridotite. The other symbols plotted are residues of reactive crystallization between peridotite and melt derived from low to moderate degree of partial melting of recycled oceanic crust with various proportion of CO2, from 0 wt.% (NA, Mallik and Dasgupta, 2012) to 5 wt.% (BAC, Mallik and Dasgupta, 2014, 2013) at 2.5 - 3 GPa. The percentage next to the symbols represent the initial proportion of melt to peridotite.

A high melt to rock proportion would result in the consumption of olivine and melt to crystallize pyroxene, with remaining partial melt that is less siliceous and more Mg-rich than the partial melt of the heterogeneity. A low melt to rock proportion would result in complete crystallization of the partial melt to form pyroxene, with residual olivine from the peridotite. Similar reasoning can be made with other heterogeneity compositions: silica deficient pyroxenites will result in olivine production at the expense of orthopyroxene, but for a low melt-rock ratio, the melt will be consumed during the reaction (Lambart et al., 2012). Thus, such a process of reactive crystallization between partial melt from a heterogeneity and peridotite not only produces distinct residual partial melt compositions, but also contributes to further heterogeneity in the upper mantle **(Fig. 5d)**. Due to the interaction of heterogeneities with peridotite, such melt-rock reactions may occur beneath mid-ocean ridges (Borghini et al., 2017; Lambart et al., 2012), ocean islands (Mallik and Dasgupta, 2012, 2013, 2014; Sobolev et al., 2005), continental lithosphere (Chen et al., 2017; Kiseeva et al., 2013), in subduction zones near depths of arc magma generation (Kelemen, 1995; Mallik et al., 2015, 2016; Prouteau et al., 2001; Tatsumi, 2001; Wang and Foley, 2018), and as deep as the transition zone (Kiseeva et al., 2013; Thomson et al., 2016).

4 Sampling melts of the mantle - approach and overview

In this section, we present a brief, and by no means comprehensive, survey of the magma generation processes and compositions of natural samples from three tectonic settings on Earth: mid-ocean ridges, ocean islands, and volcanic arcs. For each setting, we review experimental constraints on magma genesis, followed by a discussion of the compilation of natural compositional data. To facilitate as many comparisons between experimental data and natural data across the three settings, we focus exclusively on major element compositions. Obviously, using only major elements rather than emphasizing only primitive samples presents limitations for fingerprinting the nature of the melting source. Our goal here is not to identify the source characteristics, since trace element ratios and isotopes would be better suited for that task, but to make broad comparisons between experimental, modeling, and natural observations in terms of petrogenetic processes across the major tectonic settings of magmatism on Earth.

Supplementary Data and literature sources used in this review are summarized in Table S1 and are all reported in **Supplementary Tables S6, S7 and to S8**. Owing to the extremely large number of samples, particularly for arc volcanic rocks (nearly 40,000), we contoured all the volcanic rock data using a smoothed histogram method (Eilers and Goeman, 2004), using 75 histogram bins in the x and y direction and a positive smoothing parameter (λ) of 1.5 (higher values of λ lead to more smoothing; a value near zero would result in a plot of essentially the raw data). Density contours for volcanic rocks in **Fig. 6** were constructed at intervals of 10%. We applied the same parameters in the contouring for the volcanic rock data from each tectonic setting so side-by-side comparisons can be accurately made. Owing to the small number of plutonic cumulate rocks (<500 at any given setting) and melt inclusions (<200, from volcanic arcs only), we did not contour these datasets.

4.1 MORB

4.1.1 Intracrustal processing.

The relatively simple geodynamic setting of mid-ocean ridges serves as a baseline model for mantle melting and magma generation. A primary magma is one formed during adiabatic decompression melting of mantle peridotite and which has not been modified during ascent and eruption. It has long been recognized that such a magma is rarely, if ever, sampled at mid-ocean ridges (or any tectonic setting for that matter) – the average Mg# of all MORB is 56, significantly lower than the value of ~70 expected for equilibrium with mantle peridotite. Three main factors are involved in producing the compositional spectrum of mid-ocean ridge basalts (MORBs): 1) mantle source heterogeneity, 2) style of mantle melting, and 3) intracrustal processing. In this section, we focus on the role of intracrustal processing, which marks the boundary between the melting regime and the onset of crystallization, differentiation, eruption and eventual sampling.

In order to go from sampled MORBs from the seafloor to how such MORBs looked when they parted ways with the mantle, the contributions from crystallization-differentiation, which occur in the crust must first be understood. Intracrustal processing of MORB can be broadly considered as variations on the theme of fractional crystallization (FX). The simplest scenario, and, today, the paradigm, is that MORB follow a differentiation path under anhydrous, low pressure conditions, evolving towards the classic Fe-enrichment (tholeiitic) trend (O'Hara, 1965). Experiments and observations of natural MORBs indicate the generalized low-pressure crystallization sequence of olivine → olivine + plagioclase → olivine + plagioclase + clinopyroxene → plagioclase + clinopyroxene + orthopyroxene + Fe-Ti oxides (Coogan, 2014; Grove et al., 1993). However, detailed study of MORB over the past decades reveal several inconsistencies with the simple FX model: 1) phenocryst assemblages in MORB are not representative of cotectic proportions as predicted by FX (Francis, 1986), 2) FX models require fractionation of clinopyroxene, but it is not commonly observed as a phenocryst, and 3) some incompatible elements, like Th, are overly enriched in global MORB compared to predictions from simple fractional crystallization (Coogan and O'Hara, 2015; Jenner and O'Neill, 2012). Thus, more complex scenarios have been hypothesized to explain the mismatch between trace element data and simple fractional crystallization models. The two major variations on the simple fractional crystallization model are 1) in situ crystallization, where crystallization of a magma occurs in a progressive solidification front and involves return of interstitial melt to the magma chamber (Coogan and O'Hara, 2015; Langmuir, 1989; McBirney and Noyes, 1979) and 2) "RepTapFrac", wherein a magma chamber is periodically replenished (Rep), melt extracted (Tap), and then fractionally crystallized (Frac) (Albarede, 1985; O'Hara, 1977; O'Neill and Jenner, 2012). Additionally, recent studies suggest an alternative – reactive porous flow/melt-rock reaction – as another mechanism that could reconcile several of the MORB conundrums, particularly the observed over-enrichment in incompatible trace elements (Coumans et al., 2016; Gao et al., 2007; Lissenberg and MacLeod, 2016; Lissenberg et al., 2013). Although trapped melt and melt-rock reaction (Lissenberg and Dick, 2008) in the lower crust and even the oceanic mantle lithosphere are increasingly recognized as additional processes contributing to MORB compositional evolution (especially in the case of incompatible trace elements), the evolved nature of MORB (Mg# ~56) compared to primary mantle melts (Mg# ~70) and the overall fractionation of incompatible elements between lower oceanic crust and upper oceanic crust (Coogan, 2014) still broadly support a fundamental role for crystal-liquid separation in MORB petrogenesis.

4.1.2 Natural MORBs & their cumulates.

The perspective on MORB and oceanic crust generation has been largely focused on extrusive rocks due to accessibility – there are several thousands of samples of MORB (pillow lavas, glasses) but far fewer samples of complementary subcrustal MORB cumulates **(Table S5).** A coupled perspective of both MORBs and their cumulates can also be illustrative of the factors involved in MORB evolution. In **Figure 6a-d**, we plot both global MORBs (both lavas and glasses from the database of (Gale et al., 2013)) and a recently compiled global MORB cumulate database (Chin et al., 2018) in Harker-style diagrams. Compared to other tectonic settings (discussed in later sections), the combined global database of MORBs and MORB cumulates collectively fall on tight, minimally scattered compositional trends. Throughout a wide range of Mg# (and thus differentiation index), the SiO_2 content of MORBs remains relatively constant at ~55 wt.% **(Fig. 6a).** Crystal fractionation of olivine, followed by olivine + albitic plagioclase, is apparent in plots of Al_2O_3 vs. Mg# **(Fig. 6b)** and Na_2O vs. Mg# **(Fig. 6c).** The consistently low K_2O vs. Mg# trend of MORB cumulates **(Fig. S1)** also suggests that crystal-liquid segregation is generally efficient (Natland and Dick, 1996). Finally, the classic tholeiitic magma series is revealed in the cumulate counterparts of MORBs – the Fe-enrichment trend of MORB is balanced by the Fe-poor nature of early MORB cumulates, and the late precipitation of Fe-Ti oxides in oxide gabbros is clearly shown in a marked increase in TiO_2 at Mg# ~50 **(Fig. 6d)** (Chin et al. 2018). To first order, major element systematics of MORB + MORB cumulates supports crystal-liquid segregation along tholeiitic differentiation trends. Yet, additional observations, such as reaction textures and complex zoning patterns (Lissenberg and MacLeod, 2016), isotopic heterogeneity (Lambart et al., 2019), and phase assemblage disequilibrium (Gillis et al., 2014) in associated cumulates, seem to prevent petrologists from establishing a clear genetic link between them and MORB exclusively through fractional crystallization. While a summary of trace element systematics of MORB and MORB cumulates is beyond the scope of this study, conflicts persist as to the roles of melt-rock reaction, secondary melt infiltration - as shown by trace element studies - versus fractional crystallization, which is broadly supported by major element trends.

4.1.3 Primary MORB.

Co-variations observed in MORB suites of isotopic ratios of heavy elements (e.g., Sr, Nd, Pb, Os, Hf), being insensitive to melting and fractionation processes, are usually attributed to mantle heterogeneity (Hofmann, 2003). Additionally, timing constraints from U-series disequilibria suggest that melt extraction from the mantle is rapid (Elliott & Spiegelman, 2003; Elkins et al., 2019 and references therein). It has been suggested that high-permeability channels from the melt source region toward the surface must exist (Kelemen et al., 1995) to satisfy these constraints. Numerical models (e.g., Weatherley and Katz, 2012, 2016) show that the formation of these channels would be facilitated by the presence of lithological heterogeneities in the mantle owing to thermal interaction between partially molten and subsolidus lithologies.

To decipher source signals, MORB need to be corrected for crystal fractionation. Once corrected for low-pressure fractionation (Klein and Langmuir, 1987), MORB show evidence for variability in major-element compositions, likely due to compositional (e.g., Niu and O'Hara, 2008) or thermal (e.g., Dalton et al., 2014; Langmuir et al., 1992; Gale et al., 2014) variability in the

source. However, Neave et al. (2019) recently showed that the major element composition of a primitive magma also affects the efficiency with which it crystallises.
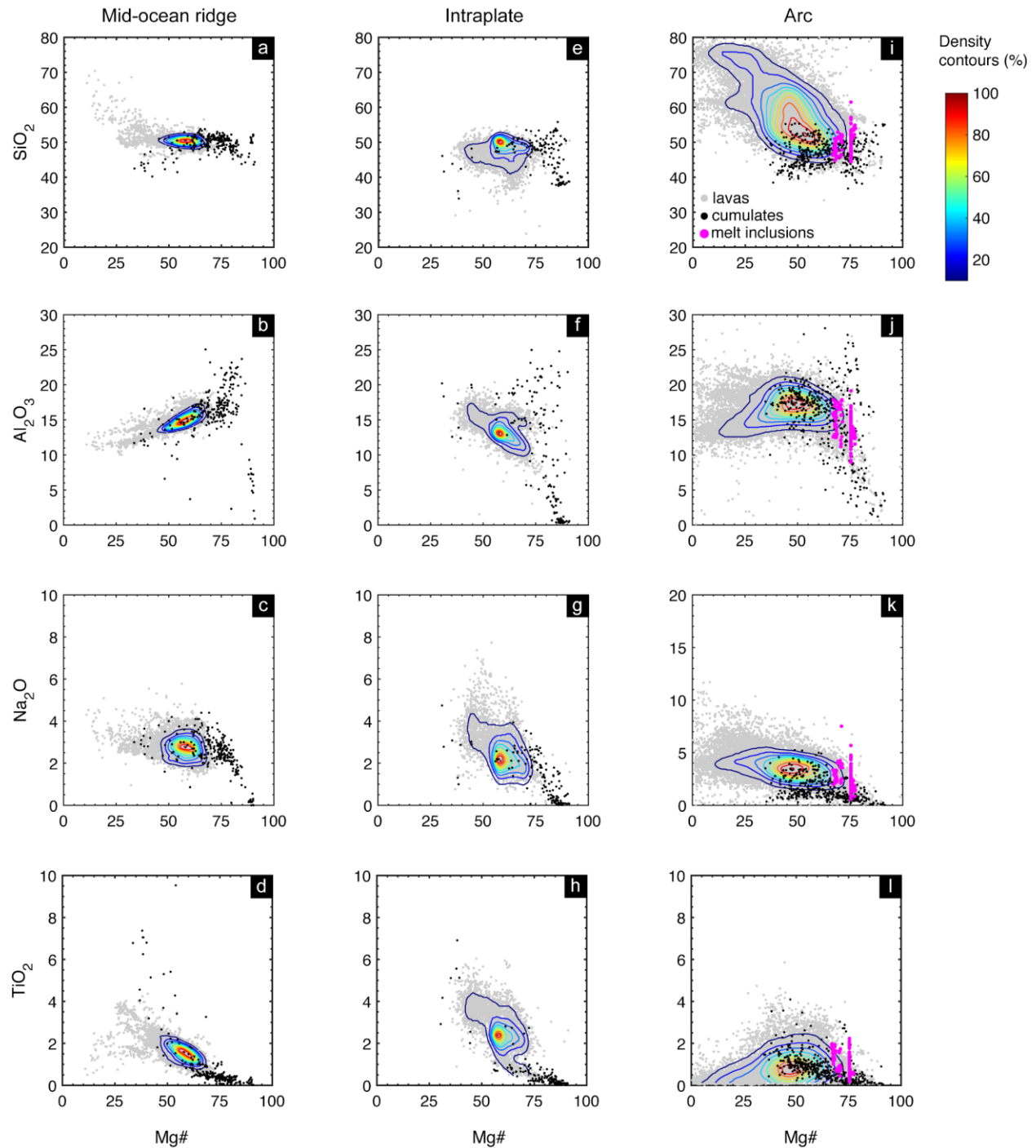
Figure 6. Major element oxides (wt.%) vs. Mg# for lavas (gray circles), cumulates (black circles), and melt inclusions (magenta symbols, from volcanic arcs only). Colored curves show the density contours (at intervals of 10%) for volcanic rocks.

Additionally, Bennett et al. (2019) demonstrated that the vertical extent of mid-ocean-ridge magmatic systems is not restricted to the first few kilometers as previously thought, but could extend down to the base of the lithospheric mantle. Thus, predominantly shallow-level fractional

crystallization of MORB may be more complex than commonly thought. Finally, in comparison to ocean island and arc basalts, the range of primary MORB major-element compositions stays restricted. This restricted variability can be explained by significant low-pressure magma mixing (e.g., Shorttle, 2015; Lambart et al., 2019), and/or by similar melting reactions and melt compositions generated by pyroxenites and peridotites in the melting zone beneath mid-ocean ridges (e.g., Lambart et al., 2009).

It is beyond the scope of this short section to discuss all of these contributing factors to MORB geochemistry in detail and we refer the reader to comprehensive reviews on MORB petrogenesis in the literature (Gale et al., 2014; Langmuir et al., 1992; Lissenberg et al., 2019; Niu and O'Hara, 2008; Rampone and Hofmann, 2012; White and Klein, 2014).

4.2. Oceanic Island Basalts

Ocean island basalts (OIB) have received considerable attention in the literature given their potential as a proxy to unravel the composition and thermal state of the mantle. Isotopic and trace element diversity in ocean island basalts are indicative of chemically heterogeneous sources such as the presence of enriched and depleted mantle reservoirs, recycled oceanic crust, continental crust and sediments. The readers are referred to the seminal reviews by Hofmann (1997, 2003) for details on how geochemical characteristics of oceanic basalts give us insight into the dynamics of the mantle.

4.2.1 Source lithologies of primitive OIB

Evidence for presence of recycled material in the mantle source of OIB come from major-, trace-element and isotopic compositions. In fact, previous studies have argued that the high TiO_2 contents (> 2.5 wt.%) of primary OIB are indicative of the presence of recycled oceanic crust in the source (**Fig. 6f**; Prytulak and Elliott, 2007). In addition, OIB compositions extend to very low silica contents (**Fig. 6e**) and primary magma with very low SiO_2 concentrations (≤ 46 wt.%) also display the highest $^{206}Pb/^{204}Pb$ ratios, indicative of recycled crust in the source (Jackson and Dasgupta, 2008). Such low SiO_2 contents are observed in experimental partial melts of recycled heterogeneities such as silica-deficient pyroxenites (Hirschmann et al., 2003; Kogiso et al., 2003; Lambart et al., 2009) and carbonated oceanic crust (Mallik and Dasgupta, 2014). However, most partial melts of recycled heterogeneities do not reach Mg# 73 (Kogiso et al., 2004; Pertermann and Hirschmann, 2003b). Such high Mg# can be explained if both pyroxenite- and peridotite-derived melts contribute to OIB genesis or if the pyroxenite-derived melt reacts with the peridotite before directly contributing to magma genesis (Sobolev et al., 2005,2007; Mallik and Dasgupta, 2012, 2013, 2014; Phipps Morgan, 2001). In fact, the process of reactive crystallization as a consequence of such a reaction between pyroxenite (eclogite)-derived melt and peridotite is described in Section 3 and results in MgO enrichment and SiO_2 depletion of the eclogite melt. In summary, it is widely accepted that the mantle source of OIB is heterogeneous, but the lithological nature and chemical composition of this heterogeneity is still debated (e.g., eclogite, pyroxenite, hybrid lithologies, refertilized peridotites). However, the compositions of the various mantle components control their contribution to magma genesis by affecting their melt productivity (Lambart et al. 2016) and reactivity with the surrounding mantle (Lambart et al., 2012; Mallik and Dasgupta, 2012, 2014; Sobolev et al., 2005).

To illustrate the importance of the mode of participation of the heterogeneities in the source of OIBs and their compositions, we perform an exercise as described below. We remind the readers that the primary goal of this exercise is to highlight the effects of the choice of the melting model, and less to quantify the proportion of pyroxenite in the mantle source of OIB. We first consider a simple case where deeper melt derived from recycled crust is channelized through the peridotite matrix (dashed region in **Fig. 5a, b**) and mixes with peridotite partial melt at shallower depths to produce the observed primary magma compositions. We call this the 'melt-melt mixing model'. In this model, melt-rock interactions are not taken into account. We consider two pyroxenite compositions: G2, a MORB-type eclogite (Pertermann and Hirschmann, 2003a) and MIX1G, the average natural pyroxenite (Hirschmann et al., 2003), and estimate their proportions in the sources of ocean islands globally as follows: we use the primary melt compositions and LAB (Lithosphere – Asthenosphere boundary; proxy for the final depth of melting) thicknesses at the time of volcanism for each individual ocean island as reported by Dasgupta et al., (2010) and we use PRIMELT3 MEGA.XLSM software (Herzberg and Asimow, 2015) to estimate the potential temperature (T_P) for each island. As described in Section 2, the melts derived from eclogitized crust (or any lithologies dominated by clinopyroxene and garnet) would have a lower Mn/Fe than partial melts of peridotite or high Mg-pyroxenite containing olivine and/or orthopyroxene. Thus, olivines that would crystallize from a melt with contributions from clinopyroxene and garnet bearing pyroxenites would also mirror the low Mn/Fe signatures. Sobolev et al., (2007) used this observation to derive an empirical relationship between Mn/Fe of olivines in equilibrium with primary basalts and the contribution of pyroxenite in the aggregate basaltic melts (X_{melt}^{pyr}):

$$X_{melt}^{pyr} = 3.48 - 2.071 \times (100Mn/Fe) \qquad (2)$$

We note that Matzen et al. (2017b) demonstrated that the Mn content variation in early crystallizing olivines can be explained by partial melting of peridotite over a range of pressures, and that recycled lithologies may be present in the source but are not required to explain the Mn variations in olivines. However, the goal of the following exercise is to simply demonstrate that the estimated proportion of pyroxenite in the mantle source of OIBs varies with the choice of melting model and composition of pyroxenite.

With the PRIMELT3 MEGA.XLSM software, we calculated the Mn/Fe ratio of the olivine in equilibrium with the primary OIB and used Sobolev's proxy to estimate X_{melt}^{pyr} from the ocean islands. Finally, the proportions of pyroxenites in the source of the ocean islands (X_{source}^{pyr}) are calculated using Melt-PX (Lambart et al., 2016) and assuming the following relation that includes a first-order assumption that the proportion of pyroxenite in the melt is weighted by the abundance of pyroxenite in the source:

$$X_{melt}^{pyr} = \left(X_{source}^{pyr} \times F_f^{pyr}\right)/\left(X_{source}^{pyr} \times F_f^{pyr} + \left(1 - X_{source}^{pyr}\right) \times F_f^{per}\right) \qquad (3),$$

with F_f^{pyr} and F_f^{per}, the final degree of melting of the pyroxenite and the peridotite, respectively, when the parcel of upwelling mantle reaches the LAB.

In a second set of calculations, we use the same constraints on T_P and P_f, but consider that melt derived from G2 first reacts with the peridotite before contributing to magma genesis (e.g., Sobolev et al., 2005). We call this the 'reactive crystallization model'. Mallik and Dasgupta (2014) used published experimental results to derive an empirical relation that predicts the major element concentrations in a primary melt that forms by reactive crystallization of partial melts

from eclogite-derived crust (similar to G2) as they undergo porous infiltration through a subsolidus peridotite matrix. While the proxy of Sobolev et al. (2007) is based on the trace element compositions in olivine (equation 1), Mallik and Dasgupta's model is based on the major element composition of the primary magmas. Using two independent models allows us to test for the consistency of such empirical relationships. In Mallik and Dasgupta's model, melt-derived from the recycled crust reacts with the peridotite to form a hybrid lithology and a distinct melt. The distinct melt is in chemical and thermal equilibrium with the hybrid lithology, and this melt, by mixing with peridotite-derived melt results in the observed primary magma composition. The empirical relation of Mallik and Dasgupta provides the fraction of recycled crust-derived melt required to produce the new hybrid lithology (X^{rl}), and the proportion of melt derived from the hybrid lithology (X_{melt}^{hyb}). Using these, we can estimate the proportion of G2 (before melting) in the source using the following equation (Sobolev et al., 2005)

$$X_{source}^{G2} = \frac{X^{rl}}{F^{G2} \times \left(\frac{1-X_{melt}^{hyb}}{X_{melt}^{hyb}} \times \frac{F_f^{hyb}}{F_f^{per}} + \frac{1-F^{G2}}{F^{G2}} \times X^{rl} + 1 \right)} \qquad (4),$$

where, $F^{G2} (= 8.9 \text{ wt.\%})$ is the melting degree undergone by G2 before reacting with the surrounding mantle, and F_f^{hyb} and F_f^{per}, the melting degrees of the hybrid lithology and the peridotite calculated with Melt-PX when the mantle parcel reaches P_f. **Fig. 7** presents estimated X_{source}^{pyr} for each major group islands in the three oceans for the two models of melting. Calculations have been performed on individual islands listed in Dasgupta et al. (2010) (see **Supplementary Table S9**). To facilitate the comparison, we report the results averaged by island groups and the error bars show the variability between islands from the same group. Hence, a group with only a single island, such as Iceland, has no error bars. The proportion of pyroxenites in the mantle source significantly varies between the type of calculations, but also between and within each island group. Using the 'melt-melt mixing model' and the composition G2, the average proportion of pyroxenite in the source contributing to OIB genesis is ~34 % and varies from 8% (Balleny) to 100% (Tristan da Cunha and Gough). Due to its higher solidus temperature than G2 (Lambart et al., 2016), using the composition MIX1G results in an overall higher proportion of pyroxenite in the source required to explain the Mn/Fe ratio (~54% in average). Proportions of G2 estimated with the 'reactive crystallization model' vary from 0% (Iceland and Amsterdam) to 61% (Cameroon and Fernando de Norhona). In summary, despite constraints on the mantle temperature and final pressure of melting, the choice of the model and composition of the enriched component/heterogeneity will significantly affect the estimates of its proportion in the mantle source of magmas. Despite these discrepancies, these models converge to the conclusion that a large fraction [39 (± 28)%] of recycled material is present in the mantle source of OIB .
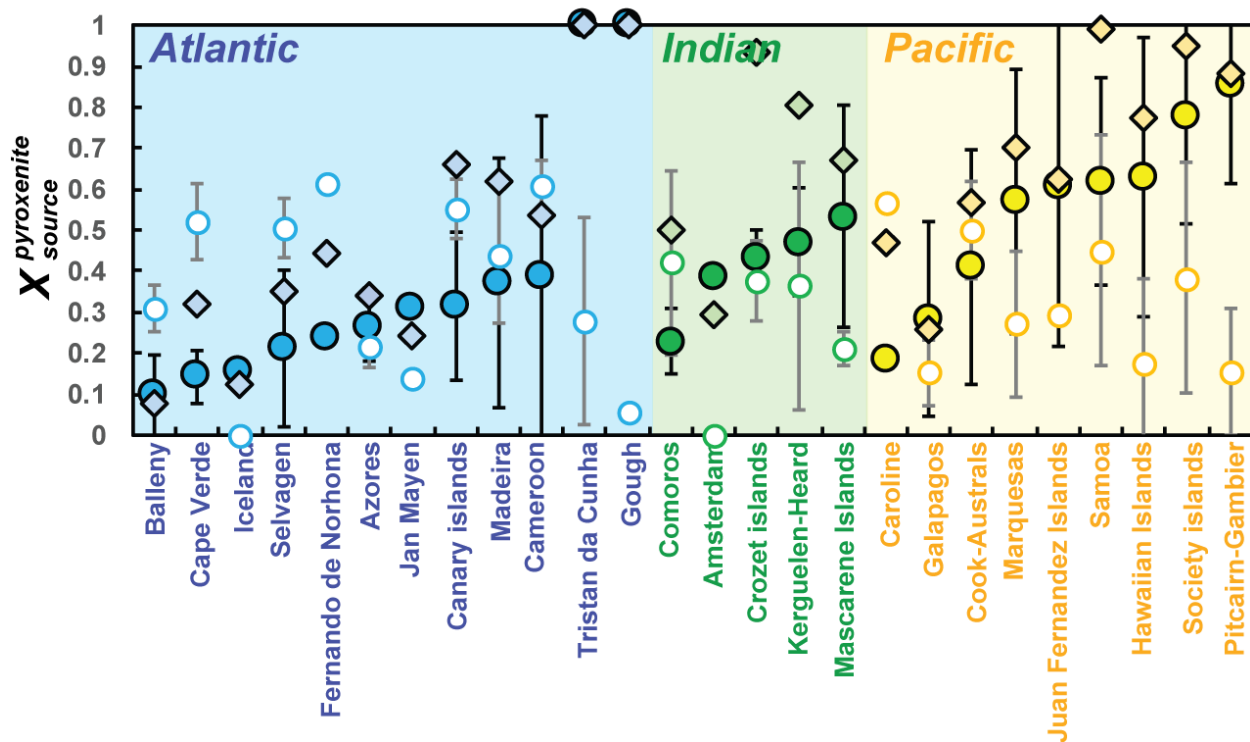
Figure 7. Calculated average proportions of pyroxenite in the source of the main island groups using a simple melting model ('melt-melt mixing model') with either G2 (filled circles) or MIX1G (diamonds) as pyroxenitic component and using a 'reactive crystallization model' using G2 (open circles) as pyroxenitic component. The error bars on G2 fractions correspond to one standard deviation on each island group calculated from fractions obtained for individual island (Table S9). (Black and grey error bars show variability inside each island group calculated using the melt-melt mixing model with G2 and using the reactive crystallization model, respectively).

We also note there is no strong correlation between the estimated proportion of pyroxenite in the source and T_P **(Fig. 8a)** or LAB thickness (also P_f ,**Fig. 8b)**. This result contrasts with Sobolev et al.'s (2007) conclusions suggesting that more energetic (i.e., hotter) plumes were more likely to carry a large amount of recycled crust into the upper mantle due to higher buoyancy. However, it is worth noting that the model of Herzberg and Asimow (2015) assumes a peridotite source. Herzberg and Asimow (2008) pointed out that if the mantle source contains pyroxenite and/or volatiles, it might result in overestimation of the calculated potential temperatures by ~100°C. This is consistent with Mallik and Dasgupta (2014) who showed that an OIB source with 120-1830 ppm CO_2 (Dasgupta and Hirschmann, 2010) translate to an excess estimation of T_P between 2 and 73 °C (assuming 5-10% partial melting at the source and incompatible behavior of CO_2 during partial melting). This calls for a recalibration of mantle thermometers in the future, to take into account the effects of a heterogeneous and volatile-bearing mantle. In fact, a higher T_P will result in a lower contribution of the pyroxenite component in the magma (**Fig. 3**). In other words, overestimating the potential temperature will also result in an overestimation of the pyroxenite fraction required in the source for a given proportion of pyroxenite in the magma. Nevertheless, consistent estimates for the potential temperatures for Hawaii and MOR by other independent methods, such as calibrating major element compositions of liquids with temperature (Lee et al., 2009; Purtika, 2008), suggest that this temperature overestimation is

limited and support the decoupling between the thermal state of the lithosphere and the amount of recycled material in the mantle.
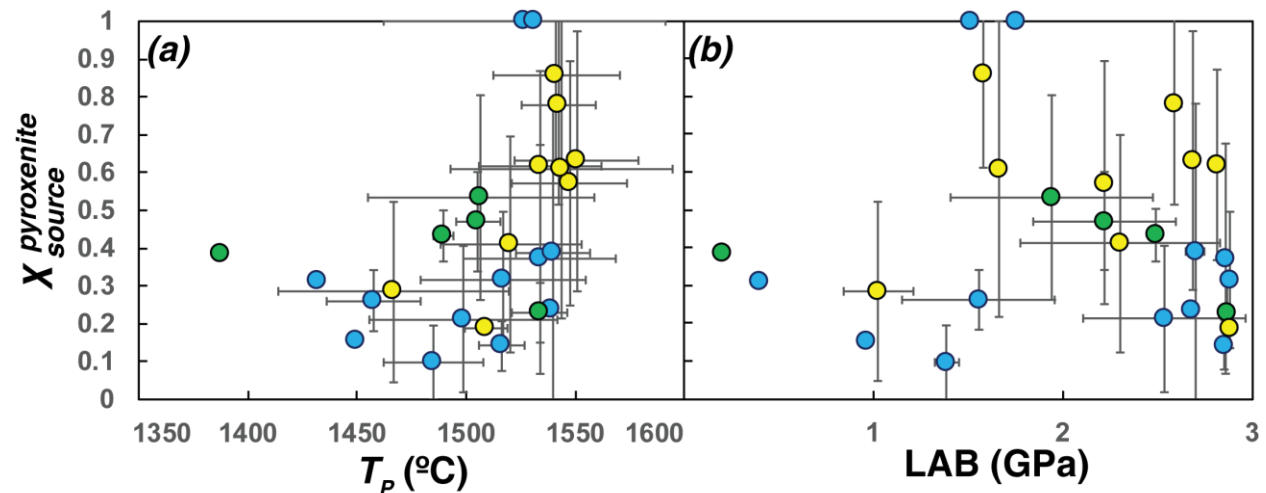
Figure 8. Calculated average proportions of G2 using the simple melting model (first set of calculations) as a function of the average T_P (a) and the average pressure of the LAB (b). Same color code as in **Fig. 7**. The error bars correspond to the standard deviation on each island group calculated from fractions obtained for individual island.

4.2.2 Natural OIB & their cumulates

OIB display a wider range of major element compositions compared to MORB, but not nearly as wide and variable as arc lavas **(Fig. 6).** Both MORB and OIB show a population density peak around Mg# = 55, suggesting similar degrees of crystal fractionation. Thus, we could infer that the fractionation process for MORB and OIB are relatively similar and the larger range of compositions displayed by OIB is not due to fractionation processes, but instead reflect a larger variability in primary magma compositions. In detail, major element trends of OIBs differ from MORB trends in the following ways: 1) OIB compositions extend to lower SiO_2 over similar Mg# intervals compared to MORB**,** 2) OIBs have higher TiO_2 (>2.5 wt.%) than MORB (~2 wt.%), and much higher than arc lavas (<2 wt.%) , 3) Fe-enrichment is not as extreme in OIB as it is for MORB, 4) OIBs follow a trend of Al_2O_3 enrichment with decreasing Mg#, whereas MORB become depleted in Al_2O_3 , 5) OIBs achieve higher and more variable Na_2O and K_2O contents compared to MORBs **(Fig. 6, Supplementary Fig. S1)**. The spread in FeO_T, Al_2O_3, Na_2O, and K_2O in OIBs versus MORBs likely reflects larger variability in primary OIB magma compositions. Part of this contrast of variability between OIB and MORB is due to the extensive magma mixing at mid-ocean ridges that significantly restricts the range of primitive compositions displayed by MORB (Batiza, 1984; Cipriani et al., 2004). In all the binary oxide plots **(Fig. 6, middle panel)**, the contoured OIB data are skewed toward higher Mg# values compared to MORB, and (near-) primary magmas are commonly sampled, suggesting more limited mixing in oceanic island settings. In addition, and as previously noted, pyroxenites and peridotites produce melt with very similar major element compositions at pressures relevant for mid-ocean ridges (i.e., 1-1.5 GPa, Lambart et al., 2009; Borghini et al., 2017). However, at higher pressures, pyroxenite melting relationships are controlled by the presence of the pyroxene-garnet thermal divide (Kogiso et al., 2004) and can produce highly contrasted melt compositions. Hence, the same amount of lithological heterogeneity in the mantle source results

in a higher diversity of magma compositions in OIB settings than in MORB settings. The silica-poor OIB compositions, for instance, are consistent with the partial melting of Si-deficient pyroxenites at high pressure (Hirschmann et al., 2003). As previously mentioned, the high TiO_2 contents are also consistent with the presence of recycled oceanic crust in the OIB source.

Finally, the sources of OIBs are usually assumed to be more heterogeneous than the mantle source of MORBs, mostly because primary OIBs also display larger variability in trace element and isotopic ratios than MORBs (Hofmann, 1997, 2003). Two causes for OIBs being more heterogeneous in their source than MORBs are proposed as follows. OIBs show a wider range of T_{PS}, spanning to higher T_{PS} than that of MORBs **(Fig. 5a),** and a hotter mantle may result in increased thermal buoyancy of dense garnet-bearing heterogeneities, and therefore, easier for such heterogeneities to accumulate within the upper mantle source of the OIBs (Brown and Lesher, 2014; Sobolev et al., 2005). Also, a thicker lithosphere beneath OIBs, and therefore a higher final pressure of melting, may preserve the chemical signature of heterogeneities better due to lesser degree of partial melting of peridotites (Sobolev et al., 2007). However, we do not observe any correlation between the proportion of chemical heterogeneity and T_P or P_f **(Fig. 8)**, implying that the thermal state of the mantle and the proportion of mantle heterogeneity are decoupled. This casts doubt on the above two propositions about why MORBs may have less heterogeneous sources than OIBs. Ultimately the answer may lie in the process of melt generation such that MORBs undergo greater magma mixing than OIBs (e.g. Zindler et al., 1984), resulting in a tighter range in the concentrations of trace elements and isotopic ratios, and the presence of variability in geochemical signatures in OIBs (or their lack in MORBs) may not be an indicator of how heterogenous their sources are.

4.3. Arc magmas

4.3.1 Arc magma genesis - a complexity of factors

Compared to the relatively simple geometry of spreading centers at mid-ocean ridges and the non-tectonic origin of OIBs, the geodynamic setting of volcanic arcs is far more complex, involving multiple moving parts: a hydrated downgoing plate, a convective mantle wedge continuously fluxed by volatiles from the downgoing plate, and overriding plate lithosphere, which itself may be old and heterogeneous (e.g. at continental arcs). As a result, arc magmas worldwide show incredible compositional diversity compared to MORBs and OIBs, reflecting the interplay of the different tectonic components involved. Arc magmas range from basalts (40 – 52 wt.% SiO_2) to rhyolites (>70 wt.% SiO_2) **(Fig. 6i)**. Mg#'s of arc volcanic rocks range from <10 to ~80 **(Fig. 6, right panel).** Such compositional variation is attributed to both primary processes – e.g. those involving melting and melt-rock interaction of peridotitic source rocks in the mantle wedge (and generation of primary melts *sensu stricto*), and secondary processes – such as fractional crystallization and assimilation of pre-existing crust. In addition, there is increasing recognition that partial melting and involvement of non-peridotitic source rocks, such as the downgoing, metamorphosed oceanic slab and sediments, may also contribute to arc magma genesis (as discussed in section 4.3.3). Below, we review experimental constraints on primary melt generation in arcs, discuss recent advances in non-peridotitic contributions to arc magmatism, and summarize key major element compositional trends in natural arc magmas and their cumulates.

4.3.2 Experimental perspectives on primary arc magma generation: melting of the peridotitic mantle wedge

We will first investigate the formation of primary arc magmas derived from the peridotitic mantle wedge. The geodynamic scenario for such melting, which constitutes the majority of arc magmatism, is devolatilization of the downgoing slab which induces hydrous flux melting of the dominantly peridotitic mantle wedge (Grove et al., 2006; Till et al., 2012). The chemistry of primary arc magmas depends on the pressure-temperature conditions of partial melting in the mantle, composition of sub-arc peridotite and slab fluxes, and the H_2O content, and oxygen fugacity at the source of melting. Previous experimental studies have investigated the effect of H_2O on partial melting of peridotite (e.g., Gaetani and Grove, 1998; Grove et al., 2006; Hirose, 1997; Hirose and Kawamoto, 1995; Tenner et al., 2012; Till et al., 2012), and mixtures of hydrous siliceous crustal melt and peridotite (Mallik et al., 2015, 2016; Pirard and Hermann, 2014, 2015; Prouteau et al., 2001; Rapp et al., 1999). The partial melts span a wide range in total alkali-silica space covering the entire spectrum of primary arc magmas from basaltic to andesitic and basaltic trachy-andesitic **(Fig. 9a).**

Given the importance of H_2O in subduction zone magmatism, it is important to constrain the effect that H_2O has on the chemistry of magmas produced in the sub-arc mantle and experiments investigating partial melting behavior of the sub-arc mantle can give us insight into this. Experimental melt compositions that co-exist with both olivine and orthopyroxene (the two most abundant minerals in the upper mantle) are compiled and their H_2O contents are plotted against their silica contents **(Fig. 9b).** Two trends emerge. Melt compositions produced at pressures lower than 2 GPa show increasing silica contents with H_2O, whereas, for melt compositions produced at pressures greater than 2 GPa, silica contents are anti-correlated with H_2O **(Fig. 9b).** This observation indicates that pressure and H_2O contents affect the chemistry of partial melts, and approach towards the development of a model of subduction zone melting requires that we understand the reason behind such a trend. Mallik et al. (2016) explained that the increasing SiO_2 trend at lower pressures is caused by the expansion of olivine stability over orthopyroxene with H_2O. The reverse trend at higher pressures is caused by an expanded orthopyroxene stability field over olivine. Thus, future development of a holistic model of partial melting of the mantle in subduction zones requires in-depth understanding of how phase equilibria are affected by such factors . While the effect of pressure, temperature and bulk composition (including H_2O content) have been investigated in previous studies, the effect of oxygen fugacity on differentiation in arcs is still debated. It has long been known that arc lavas are more oxidized than MORBs (Carmichael, 1991), but the origin of the oxidized signature remains debated. Analyses of Fe^{3+}/total Fe in primitive melt inclusions from subduction zones also indicate that arc lavas are more oxidized than mid-ocean ridge basalts and back-arcs, suggesting an origin from a mantle wedge that has been oxidized by slab-derived materials (Brounce et al., 2014, 2015; Grocke et al., 2016; Kelley and Cottrell, 2009; Tollan and Hermann, 2019). However, other studies using redox-sensitive trace elements (Lee et al., 2005; Lee et al., 2010) and isotopic constraints (Dauphas et al., 2009) challenge this hypothesis , and suggest instead that arc lavas acquired their oxidized state via fractional crystallization (Chin et al., 2018; DeBari and Greene, 2011; Jagoutz, 2010; Lee et al., 2006; Tang et al., 2018, 2019), mixing and crustal assimilation (Grove et al., 1982; Patiño Douce,1999), or upper crustal differentiation and open system processes (Blatter et al., 2013; Humphreys et al., 2015).
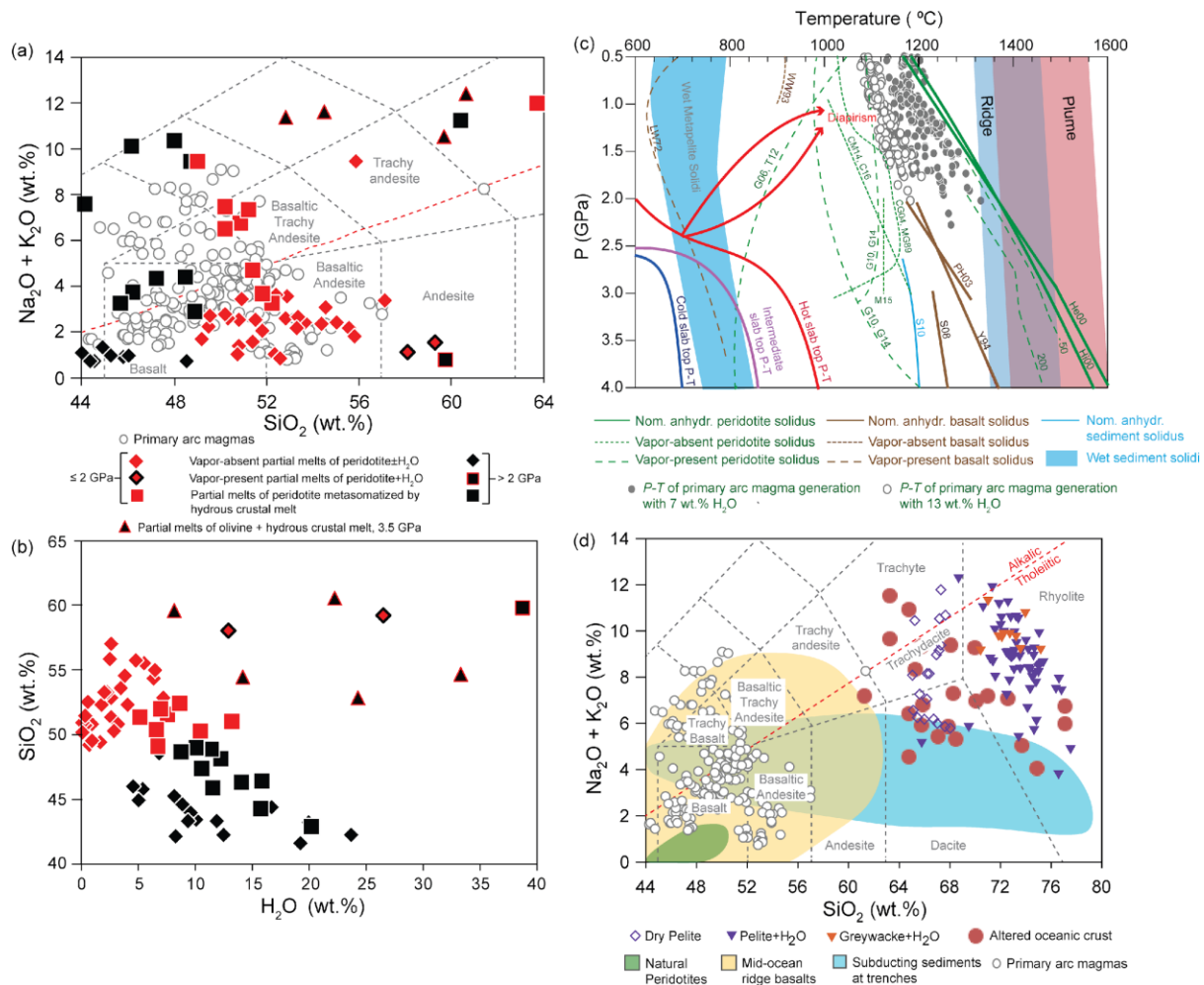
Figure 9. (a) Experimentally produced peridotite partial melts without H_2O, with H_2O but no co-existing aqueous vapor, and co-existing with aqueous vapor plotted in SiO_2 versus total alkali space . Partial melts of peridotite metasomatized by hydrous crustal partial melts are also plotted . (b) H_2O versus SiO_2 concentrations of experimentally derived partial melts in equilibrium with olivine and orthopyroxene. This subplot is a modification of **Figure 7** in Mallik et al. (2016). All compositions plotted in the subplots have been normalized to a volatile-free basis. (c) P-T space showing the solidi of nominally anhydrous peridotite, peridotite with 50 and 200 ppm H_2O, wet but vapor absent peridotite solidi, nominally anhydrous oceanic crust or basalt, vapor present basalt, wet but vapor absent basalt, nominally anhydrous sediments and wet sediments. The ridge and plume adiabats as well as the hot, intermediate and cold subduction geotherms are the same as in **Figure 5**. Primary arc magma compositions with 7 and 13 wt.% H_2O, corrected to be in equilibrium with olivine of Mg# 91 are also plotted. (d) SiO_2 versus total alkali ($Na_2O + K_2O$) space with partial melts of sediments and altered oceanic crust produced in experiments, primary arc magmas (same as plotted in panel a), and naturally occurring peridotites, mid-ocean ridge basalts and subducting sediments (are plotted. The classifications of rock types in the figure are based on Le Bas et al., (1986). For details about primary arc magma calculation and he references for the sources of data, see Supplementary Text S1.

4.3.3 Melting of non-peridotitic sources in arc magma generation.

Downgoing plate contributions to fluid flux & sediment melt diapirs. Based on the similarity of geochemical signatures between subducting sediment and volcanic arc lavas (Plank, 2005), and reproduction of the geochemistry of arc basalts by dehydration of subducted slab (sediments and hydrothermally altered oceanic crust) along with subsequent metasomatism of the sub-arc mantle (Tatsumi and Kogiso, 2003), the involvement of the subducted slab in arc magma production is well-established. Aqueous fluids released from the dehydration of subducted sediments and

altered oceanic crust lower the solidus temperatures of sub-arc mantle peridotite due to cryoscopic depression of melting temperatures by H_2O flux. Also, these aqueous fluids metasomatize or alter the mineralogy of the sub-arc mantle to produce hydrous minerals such as mica (phlogopite), amphibole and chlorite. The solidus of such metasomatized peridotites are also lower than that of nominally anhydrous peridotite **(Fig. 9c).** The latest global thermal models of subduction (Syracuse et al., 2010) show that the solidi of fluid-fluxed peridotite and metasomatized peridotite lie in the thermal regime of the mantle wedge, hence, the sub-arc mantle undergoes fluid-fluxed partial melting. However, it is interesting that fluxing fluids from the dehydration of the slab also lower the solidus of the sediments and altered oceanic crust **(Fig. 9c).** The latest global thermal models of subduction show that for intermediate subduction zones (such as Guatemala/El Salvador) and hot subduction zones (such as Central Cascadia), the aqueous fluid-fluxed solidi of sediments and altered oceanic crust intersect the pressure-temperature paths of the slabs **(Fig. 9c).** This implies that sediments and altered oceanic crust partially melt in intermediate to hot subduction zones, and the partial melts are expected to participate in primary arc magma formation. Based on geochemical proxies such as elevated Th/Yb and low Lu/Hf, contribution of slab partial melts to the source of arc magma have been inferred for Central Mexican Volcanic Belt (Cai et al., 2014), Sunda and Lesser Antilles (Woodhead et al., 2001), and the Marianas (Tamura et al., 2014) .

The following two observations can be made about partial melt of subducted crust and the dynamics of subduction zones. Firstly, the partial melts of subducted sediments and altered oceanic crust are much more siliceous ($SiO_2 > 60$ wt.%) than primary arc basalts **(Fig. 9d),** hence, by themselves cannot explain the chemistry of primary magmas produced in subduction zones. Also, the partial melts are more siliceous than partial melts derived from peridotites **(Fig. 9d).** Secondly, according to the thermal models of subduction zones, the isotherms are very closely spaced along the slab top, thus, the slab-top can be as much as 400 °C colder than the overlying sub-arc mantle within a narrow distance of less than around 25 km (Syracuse et al., 2010). These observations imply that slab-derived partial melts are colder (i.e. in thermal disequilibrium) and also chemically distinct (i.e. in chemical disequilibrium) from the adjacent sub-arc mantle. Therefore, as described before, slab partial melts undergo reactive crystallization as they react with the overlying sub-arc mantle (Johnston and Wyllie, 1989; Mallik et al., 2015, 2016; Prouteau et al., 2001; Rapp et al., 1999; Sekine and Wyllie, 1982). Previous studies have shown that such melt-rock reaction produces geochemical signatures of certain primitive arc magma types such as high Mg-andesites and dacites (Prouteau et al., 2001; Tatsumi, 2001; Kepezhinskas et al., 1996), adakites (Rapp et al., 1999) and potassic to ultra-potassic arc magmas (Mallik et al., 2015, 2016).

Geodynamics of subduction zones are further complicated by the potential for buoyant diapirs rising from the subducted slab. As shown by previous studies from geodynamic simulations and geochemistry (Behn et al., 2011; Castro and Gerya, 2008; Marschall and Schumacher, 2012; Nielsen and Marschall, 2017), a mélange comprised of physical mixtures of sediment, altered oceanic crust and metasomatized slab lithosphere can advectively ascend into the overlying hotter mantle wedge from the subducted slab, where it can partially melt and contribute to primary arc magma formation **(Fig. 9c).** Partial melting of physical mixtures of mélange-like compositions and metasomatized lithosphere have been shown to produce alkaline arc magmas (Cruz-Uribe et al., 2018) and ultrapotassic to potassic magmas in arcs and cratons (Förster et al., 2017, 2018; Wang et al., 2017). Finally, the hybridisation of the mantle wedge by

melts derived from mélange can also produce a range of primary arc magmas, from tholeiitic to calc-alkaline composition (Codillo et al., 2018).

Upper plate processes

In addition to contributions from the downgoing slab, arc magmas may also be influenced by processes in the upper (overriding) plate lithosphere. Since the seminal work of Hildreth and Moorbath (1988) in the Chilean Andes, the concept of a "MASH" (mixing, assimilation, storage, homogenization) zone in the overriding plate has become widely accepted and refined by experimental petrology and geodynamic modeling. The most recent iteration of the MASH hypothesis, Annen et al.'s (2006) Deep Crustal Hot Zone model involves both fractional crystallization of primary arc magmas in the uppermost mantle and deep crust, as well as partial melting of pre-existing crustal rocks in the upper plate. Although by no means an exhaustive list, detailed field studies of arc plutonic rocks from Kohistan (Jagoutz, 2010), Famatinian arc, Argentina (Otamendi et al., 2012; Walker Jr et al., 2015), as well as studies of deep crustal cumulate xenoliths from the Sierra Nevada, California (Ducea, 2002; Lee et al., 2006), Arizona (Erdman et al., 2016) support a primary role for crystallization-differentiation as the mechanism of growing new arc crust, and support the petrological requirement that mafic to ultramafic cumulates be the necessary complements to silicic, calc-alkaline batholiths that are the hallmark of convergent margins. Crystal fractionation of so-called "primary" arc magmas may occur even deeper than the lower crust, as evidenced by residual arc mantle lithosphere that experienced refertilization by basaltic arc melts, resulting in the precipitation of clinopyroxene and garnet ("arclogites") as the melts evolved at depth (Chin et al., 2014; Chin et al., 2016). However, similar pyroxenite enrichment can also occur via melt-rock reaction in the convecting mantle wedge (Berly et al., 2006; Green et al., 2004; Kelemen et al., 1998), and recent studies of global arc volcano trace element systematics suggest that the mantle wedge itself may be periodically metasomatized by enriched continental lithosphere that is eroded during arc magmatism (Turner and Langmuir, 2015). It is thus difficult to separate the contributions from a "contaminated" wedge vs. lithospheric components by using arc volcanic rocks and shallow plutons alone, since both experienced protracted evolution throughout the arc crust, and therefore likely record a combination of both processes (Farmer et al., 2013). Nevertheless, mass balance constraints for the bulk continental crust require at least a 2:1 (but likely to be 10:1 or more) ratio of mafic-ultramafic cumulates and restites as counterparts to the silica-rich arc/continental crust; provided those cumulates are not always convectively removed due to negative buoyancy, they make up the greatest contribution to the overriding arc crust. This, combined with the long-lived (but episodic) nature of continental arcs (Cao et al., 2017; Ducea et al., 2015), indicates that magmatic differentiation and the fractionation of massive amounts of mafic cumulates must be a primary driver of the compositional evolution of arc magmas. Thus, in addition to assimilation and partial melting of pre-existing (and usually older) crustal rocks of the upper plate lithosphere, partial melting of upper plate cumulates may also contribute to the wide variation in arc magma compositions. Foundering, eclogitized lower crust may heat up and partially melt as it descends into the mantle (Gao et al., 2004; Lustrino, 2005), providing yet another way to generate buoyant, silica-rich melts that rise up and become incorporated into the continental crust. As discussed in an earlier section, the solidus of pyroxenitic assemblages is lower than that of peridotitic ones, and so pyroxenites are more easily melted. Experimental partial melts of clinopyroxene-rich cumulates similar to those found in arcs (Médard et al., 2005) show that their

partial melts are Ca-rich and Si-undersaturated and similar to some primitive arc melt inclusions (Schiano et al., 2000).

4.3.4 Natural arc magmas & their cumulates

Erupted primary lavas in volcanic arcs are rare, as they are usually modified by secondary processes as the melt migrates from the mantle source to eruption at the surface. Direct samples of putative primary arc melts occur as melt inclusions hosted in high Mg# olivine phenocrysts. Such high Mg# (89 – 92) olivines are in equilibrium with mantle peridotite, and thus it is assumed that any liquid trapped in such olivines are also mantle-derived and therefore primary. However, olivine-hosted melt inclusions are not sampled in every arc, are not as abundant as erupted primitive lavas, and also may experience diffusive re-equilibration, potentially compromising any primary chemical signatures (Gaetani et al., 2012). In the right hand panels of **Figure 6**, we plot nearly 40,000 compositions of arc volcanic rocks downloaded from the GEOROC online database, nearly 400 cumulates of arc magmas previously compiled by Chin et al. (2018), and 205 primary arc melt inclusion compositions (see **Supplementary Table S5** for references). One of the clearest features of the data to emerge from a simple visual inspection of the major element plots is that, unlike the tightly coherent trends described by MORBs and their cumulates, arc volcanic rocks show considerable scatter and a much wider range in nearly every major element. By contrast, melt inclusions plot in a restricted Mg# window but interestingly span a wide range of compositions in certain elements, notably CaO, K_2O, and Na_2O **(Figs. 6, S1)**. Such large variations at high Mg# suggests primary melts sample heterogeneous sources in the mantle wedge and overriding plate (Sadofsky et al. 2008). Recent studies on arc lavas using trace element systematics also point to an important role of mantle wedge heterogeneity in generating the diversity of arc magma compositions (Turner and Langmuir, 2015; Turner et al., 2016). The utility of major elements in fingerprinting subduction fluxes is limited compared to the sensitivities of trace element compositions, trace element ratios, and isotopic data, but a comprehensive survey of all the available data is beyond the scope of this contribution.

As seen in the right hand panels of **Figure 6**, arc cumulates also generally span a larger compositional variation than MORB and OIB cumulates. This observation implies that arc magmas and their cumulates reflect more complex petrogenesis compared to MORBs and OIBs, as discussed earlier. For example, despite the highest concentration of arc lavas falling within a similar range of SiO_2 content as MORB and OIB (darkest red contours in **Fig. 6i**), the contoured arc lava data skew towards higher SiO_2, in contrast to MORB and OIB, the former having a more or less symmetrical distribution in SiO_2 and the latter skewing towards lower SiO_2. One explanation for the overall higher SiO_2 in arc lavas is that they experience a greater degree of fractional crystallization and/or assimilation of crustal rocks, starting at fairly primitive compositions and therefore deep and early in their evolution (Lackey et al., 2005; Nelson et al., 2013).

When arc volcanic rocks and arc cumulates are viewed together, several complementary trends consistent with an important role for fractional crystallization emerge. In the contoured data of CaO vs. Mg#, most arc volcanic rocks have CaO <10 wt.%, but MORBs have CaO >10 wt.% **(Supplementary Fig S1a,g)**. This can be explained by the early precipitation of anorthite and/or clinopyroxene as a major cumulate mineral in arcs, whereas in mid-ocean ridges plagioclase saturates early and tends to be albitic (Beard, 1986; Chin et al., 2018; Grove et al., 1993). This is also borne out in the systematics of Al_2O_3 and Na_2O **(Fig. 6j,k)**. MORB cumulates

define a tight trend in Al_2O_3 vs. Mg# space and show a peak in Al_2O_3 at high Mg# **(Fig. 6b),** whereas arc cumulates define a looser trend with a weaker peak at high Mg# **(Fig. 6j).** Indeed, the median Al_2O_3 of the most primitive MORB cumulates (Mg# 80 – 90) is substantially higher than arc cumulates in the same Mg# range (Chin et al. 2018 and **Figure 3** therein). These cumulate systematics subsequently control the Al_2O_3 content of differentiating arc magmas. In MORBs, Al_2O_3 defines a tight, decreasing trend as Mg# decreases, reflecting the simple mineralogy of MORB cumulates (gabbroic). By contrast, Al_2O_3 in arc volcanic rocks span a wide range of Al_2O_3 (10 – 20 wt.%) with decreasing Mg#, indicating multiple mineral contributions (pyroxene, amphibole, etc.) to the fractionating cumulate assemblage in contrast to the simple gabbroic mineralogy of MORB cumulates, including an important role for garnet (Tang et al. 2018), especially in continental arcs. Most arc lavas have Al_2O_3 between 16 – 18 wt.% (e.g., the classic "high alumina arc basalts", (Crawford et al., 1987)) compared to MORBs, which peak below 16 wt.% Al_2O_3, and, importantly, skew towards lower Al_2O_3 compared to arc lavas **(Fig. 6j).** The plot of Na_2O vs. Mg# also reflects the plagioclase-dominated gabbroic cumulates of MORB compared to arcs and complementary trends in the lavas. Lastly, as discussed in the MORB section, the classic tholeiitic vs. calc-alkaline trends clearly emerge in comparing MORBs vs. arcs. The diagnostic feature of calc-alkaline lavas is Fe-depletion with increasing differentiation **(Ssupplementary Fig. S1i)**, attributed to crystal fractionation of Fe- and Ti-bearing phases such as garnet and magnetite **(Fig. 6l)**.

5. Future directions

The summary of experimental data presented in Section 2 and in previous review articles (Kogiso et al., 2004; Lambart et al., 2013) emphasize the large range of compositions covered by the potential lithologies present in the mantle source of magmas. This makes it challenging to determine a unique proxy as a tracer of heterogeneities in the mantle source of magmas. In addition, calculations presented in Section 4.2 highlight that different proxies can result in different estimates of the nature and proportion of the heterogeneity in the mantle. Similarly, compositional observations of natural MORB and their cumulates point out a decoupling between the major element compositions that support fractional crystallisation as the main process of magma differentiation, and trace element compositions that indicate the strong influence of porous flow and melt-rock interactions. Hence, it is crucial for the geochemical community to concentrate their future efforts into the construction of a comprehensive dataset, with studies combining major-element, trace element and isotopic analyses. In order to correctly interpret the geochemical dataset, we need parameterizations and geochemical models that take into account such a large range of compositions. Hence, we need better constraints on the role of the lithological composition on partial melting behavior and element partitioning, especially in the presence of volatiles. As far as volatiles are concerned, the focus has largely been on H_2O and/or CO_2, but a growing consensus has emerged that other species, notably S and N are important contributors to the solid Earth volatile recycling budget (Evans, 2012; Cartigny and Marty, 2013; Mallik et al., 2018), and so also influence the partial melting behavior and consequent differentiation of the upper mantle. Future studies should not only investigate the effect of S and N, but should also constrain the effect of the presence of mixed volatile species of H-C-N-S on partial melting of the upper mantle.

As mentioned earlier in this chapter, the thermal state of the mantle, expressed in terms of potential temperature (T_P) is an extremely important aspect in the chemical differentiation of the

Earth. T_P is currently estimated based on the magnesian content of erupted primary lavas, assuming that a hotter mantle produces magmas with higher magnesia contents (e.g. Herzberg et al., 2007; Herzberg and Gazel, 2009). It has been shown that melt-rock reactions involving heterogeneities in the upper mantle and the presence of volatiles produce magnesia-rich magmas at colder mantles than that predicted earlier (Mallik and Dasgupta, 2014). This begs for further studies that would calibrate a mantle thermometer to estimate T_Ps taking into account factors such as melt-rock reactions and influence of volatiles, else we may overpredict the thermal state of the Earth's mantle beneath tectonic settings.

As far as subduction zones are concerned, there is broad agreement on the behavior of aqueous fluids and partial melts from the subducting slab and their effects on generation of arc magmas, and transfer of elements from the subducted crust to the mantle. However, one of the least understood phases in subduction zones are supercritical fluids, which are the products of complete miscibility between aqueous fluids and partial melts. The reason why supercritical fluids remain so poorly understand is due primarily to experimental difficulty in studying them. Most experimental techniques employ ex-situ analyses of samples, where the sample, after being "cooked" at the P-T of interest, are quenched to room P-T and investigated, assuming that modifications during the quenching process are not significant. Kessel et al. (2004) went a step further and cryogenically preserved the fluid in their quenched capsules during laser ablation mass spectroscopy, in order to preserve the fluid phase in their capsules. However, supercritical fluids may separate into two phases during the quenching, rendering ex-situ analyses of this phase nearly impossible. A few studies have experimentally demonstrated the closing of the miscibility gap between aqueous fluids and silicate melts under P-T conditions applicable to subduction zones (Bureau and Keppler, 1999; Kawamoto et al., 2012; Mibe et al., 2007, 2011; Ni et al., 2017; Shen and Keppler, 1997) using a Bassett-type hydrothermal diamond anvil cell or X-ray radiography using a multianvil apparatus. However, the current state-of-the-art in such in-situ experimental techniques have limitations in terms of chemical analyses that can be performed to constrain how these fluids may affect element transport in subduction zones. A future challenge for experimental geoscientists would be to improve the techniques of in-situ analysis such that supercritical fluids can be investigated better.

Finally, melt-rock interactions, in the mantle and in the crust, are increasingly recognized as important petrogenetic processes, both in the mantle and in the crust, across all geological settings. In our view, one of the major challenges faced by the experimental community is to develop tools and provide experimental constraints to predict the system behavior during these interactions including complex feedback between composition and melting and crystallization behavior and kinetics of interactions during melt transport. Some of the questions we need to address are: (1) the required conditions for the preservation of the source signal in primary magmas, (2) the effect of chromatographic melting on the range of isotopic compositions and major and trace elements concentrations in MORB and OIB (Navon and Stolper, 1987) , (3) the mechanisms of transition between the various types of magma flow in the upper mantle (porous versus focused flow; e.g., Kelemen et al., 1997), and (4) the implications of crustal melt-rock interaction on the composition of the cumulate minerals and lavas (e.g., Lissenberg et al., 2013).

References

1.   Adam, J., Green, T.H., Day, R.A., 1992. An experimental study of two garnet pyroxenite xenoliths from the Bullenmerri and Gnotuk Maars of western Victoria, Australia. Contributions to Mineralogy and Petrology 111, 505-514.

2.   Albarede, F., 1985. Regime and trace-element evolution of open magma chambers. Nature 318, 356.

3.   Annen , C., Blundy, J.D., Sparks, R.S.J., 2006. The Genesis of Intermediate and Silicic Magmas in Deep Crustal Hot Zones. Journal of Petrology 47, 505-539.

4.   Baker, M., Hirschmann, M., Ghiorso, M., Stolper, E., 1995. Compositions of near-solidus peridotite melts from experiments and thermodynamic calculations. Nature 375, 308.

5.   Baker, M.B., Stolper, E.M., 1994. Determining the composition of high-pressure mantle melts using diamond aggregates. Geochimica et Cosmochimica Acta 58, 2811-2827.

6.   Batiza, R., 1984. Inverse relationship between Sr isotope diversity and rate of oceanic volcanism has implications for mantle heterogeneity. Nature 309, 440.

7.   Beard, J.S., 1986. Characteristic mineralogy of arc-related cumulate gabbros: implications for the tectonic setting of gabbroic plutons and for andesite genesis. Geology 14, 848-851.

8.   Behn, M.D., Kelemen, P.B., Hirth, G., Hacker, B.R., Massonne, H.-J., 2011. Diapirs as the source of the sediment signature in arc lavas. Nature Geoscience 4, 641-646.

9.   Bennett, E. N., Jenner, F. E., Millet, M. A., Cashman, K. V., Lissenberg, C. J., 2019. Deep roots for mid-ocean-ridge volcanoes revealed by plagioclase-hosted melt inclusions. Nature 572(7768), 235-239.

10.   Berly, T.J., Hermann, J., Arculus, R.J., Lapierre, H., 2006. Supra-subduction zone pyroxenites from San Jorge and Santa Isabel (Solomon Islands). Journal of Petrology 47, 1531-1555.

11.   Blatter, D., Sisson, T., Hankins, W.B., 2013. Crystallization of oxidized, moderately hydrous arc basalt at mid- to lower-crustal pressures: implications for andesite genesis. Contributions to Mineralogy and Petrology 166, 861-886.

12.   Bodinier, J.-L., Godard, M., 2003. Orogenic, ophiolitic, and abyssal peridotites. Treatise on geochemistry 2, 568. doi:10.1016/B0-08-043751-6/02004-1

13.   Borghini, G., Fumagalli, P., Rampone, E., 2017. Partial melting of secondary pyroxenite at 1 and 1.5 GPa, and its role in upwelling heterogeneous mantle. Contributions to Mineralogy and Petrology 172, 70-70.

14.   Brounce, M., Kelley, K.A., Cottrell, E., Reagan, M.K., 2015. Temporal evolution of mantle wedge oxygen fugacity during subduction initiation. Geology 43, 775-778.

15.   Brounce, M.N., Kelley, K.A., Cottrell, E., 2014. Variations in Fe3+/∑Fe of Mariana Arc Basalts and Mantle Wedge fO2. Journal of Petrology 55, 2513-2536.

16.   Brown, E. L., Lesher, C. E., 2014. North Atlantic magmatism controlled by temperature, mantle composition and buoyancy, Nature Geoscience 7, 820–824.

17.   Bureau, H., Keppler, H., 1999. Complete miscibility between silicate melts and hydrous fluids in the upper mantle: experimental evidence and geochemical implications. Earth and Planetary Science Letters 165, 187-196.

18.   Cai, Y., LaGatta, A., Goldstein, S.L., Langmuir, C.H., Gómez-Tuena, A., Martín-del Pozzo, A.L., Carrasco-Núñez, G., 2014. Hafnium isotope evidence for slab melt contributions in the Central Mexican Volcanic Belt and implications for slab melting in hot and cold slab arcs. Chemical Geology 377, 45-55.

19.   Cao, W., Lee, C.-T.A., Lackey, J.S., 2017. Episodic nature of continental arc activity since 750 Ma: A global compilation. Earth and Planetary Science Letters 461, 85-95.

20.   Carmichael, I.S.E., 1991. The redox states of basic and silicic magmas: a reflection of their source regions? Contributions to Mineralogy and Petrology 106, 129-141.

21.   Cartigny, P., Marty, B., 2013. Nitrogen Isotopes and Mantle Geodynamics: The Emergence of Life and the Atmosphere–Crust–Mantle Connection. Elements 9(5), 359–366.

22.   Castro, A., Gerya, T.V., 2008. Magmatic implications of mantle wedge plumes: Experimental study. Lithos 103, 138-148.

23.   Chase, C.G., 1981. Oceanic island Pb: Two-stage histories and mantle evolution. Earth and Planetary Science Letters 52, 277-284.

24.   Chen, C., Liu, Y., Foley, S.F., Ducea, M.N., Geng, X., Zhang, W., Xu, R., Hu, Z., Zhou, L., Wang, Z., 2017. Carbonated sediment recycling and its contribution to lithospheric refertilization under the northern North China Craton. Chemical Geology 466, 641-653.

25.   Chen C.-H. and Presnall D. C., 1975. System magnesium orthosilicate-silicon dioxide at pressures up to 25 kilobars. American Mineralogist 60, 398–406.

26.   Chin, E.J., Lee, C.-T.A., Barnes, J.D., 2014. Thickening, refertilization, and the deep lithosphere filter in continental arcs: Constraints from major and trace elements and oxygen isotopes. Earth and Planetary Science Letters 397, 184-200.

27.   Chin, E.J., Shimizu, K., Bybee, G.M., Erdman, M.E., 2018. On the development of the calc-alkaline and tholeiitic magma series: A deep crustal cumulate perspective. Earth and Planetary Science Letters 482, 277-287.

28.   Chin, E.J., Soustelle, V., Hirth, G., Saal, A., Kruckenberg, S.C., Eiler, J., 2016. Microstructural and geochemical constraints on the evolution of deep arc lithosphere. Geochemistry, Geophysics, Geosystems 17, 2497–2521, doi:10.1002/2015GC006156.

29.   Cipriani, A., Brueckner, H.K., Bonatti, E., Brunelli, D., 2004. Oceanic crust generated by elusive parents: Sr and Nd isotopes in basalt-peridotite pairs from the Mid-Atlantic Ridge. Geology 32, 657-660.

30.   Codillo, E. A., Le Roux, V., Marschall, H. R., 2018. Arc-like magmas generated by mélange-peridotite interaction in the mantle wedge. Nature Communications 9(1), 2864.

31.   Coogan, L.A., 2014. 4.14 - The Lower Oceanic Crust A2 - Holland, Heinrich D, in: Turekian, K.K. (Ed.), Treatise on Geochemistry (Second Edition). Elsevier, Oxford, pp. 497-541.

32.   Coogan, L., O'Hara, M., 2015. MORB differentiation: In situ crystallization in replenished-tapped magma chambers. Geochimica et Cosmochimica Acta 158, 147-161.

33.   Coumans, J.P., Stix, J., Clague, D.A., Minarik, W.G., Layne, G.D., 2016. Melt-rock interaction near the Moho: Evidence from crystal cargo in lavas from near-ridge seamounts. Geochimica et Cosmochimica Acta 191, 139-164.

34.   Crawford, A., Falloon, T., Eggins, S., 1987. The origin of island arc high-alumina basalts. Contributions to Mineralogy and Petrology 97, 417-430.

35.   Cruz-Uribe, A.M., Marschall, H.R., Gaetani, G.A., Le Roux, V., 2018. Generation of alkaline magmas in subduction zones by partial melting of mélange diapirs—An experimental study. Geology 46 (4): 343-346.

36.   Dalton, C.A., Langmuir, C.H., Gale, A., 2014. Geophysical and Geochemical Evidence for Deep Temperature Variations Beneath Mid-Ocean Ridges. Science 344, 80-83.

37.   Dasgupta R. and Hirschmann M. M., 2010. The deep carbon cycle and melting in Earth's interior. Earth Planet. Sci. Lett. 298, 1–13.

38.   Dasgupta, R., Hirschmann, M.M., Withers, A.C., 2004. Deep global cycling of carbon constrained by the solidus of anhydrous, carbonated eclogite under upper mantle conditions. Earth and Planetary Science Letters 227, 73-85.

39.   Dasgupta, R., Jackson, M.G., Lee, C.-T.A., 2010. Major element chemistry of ocean island basalts -- Conditions of mantle melting and heterogeneity of mantle source. Earth and Planetary Science Letters 289, 377-392.

40.   Dasgupta R., Mallik A., Tsuno K., Withers A. C., Hirth G. and Hirschmann M. M. ,2013. Carbon-dioxide-rich silicate melt in the Earth's upper mantle. Nature 493, 211–215.

41.   Dauphas, N., Craddock, P.R., Asimow, P.D., Bennett, V.C., Nutman, A.P., Ohnenstetter, D., 2009. Iron isotopes may reveal the redox conditions of mantle melting from Archean to Present. Earth and Planetary Science Letters 288, 255-267.

42.   Davis, F.A., Humayun, M., Hirschmann, M.M., Cooper, R.S., 2013. Experimentally determined mineral/melt partitioning of first-row transition elements (FRTE) during partial melting of peridotite at 3GPa. Geochimica et Cosmochimica Acta 104, 232-260.

43.   DeBari, S.M., Greene, A.R., 2011. Vertical Stratification of Composition, Density, and Inferred Magmatic Processes in Exposed Arc Crustal Sections, Arc-Continent Collision. Springer Berlin Heidelberg, pp. 121-144.

44.   Ducea, M.N., 2002. Constraints on the bulk composition and root foundering rates of continental arcs: A California arc perspective. J. Geophys. Res. 107, 2304.

45.   Ducea, M.N., Saleeby, J.B., Bergantz, G., 2015. The architecture, chemistry, and evolution of continental magmatic arcs. Annual Review of Earth and Planetary Sciences 43, 299-331.

46.   Eilers, P.H., Goeman, J.J., 2004. Enhancing scatterplots with smoothed densities. Bioinformatics 20, 623-628.

47.   Elkins, L. J., Bourdon, B., Lambart, S., 2019. Testing pyroxenite versus peridotite sources for marine basalts using U-series isotopes. Lithos, 332-333, 226-244.

48.   Ellam R. M.,1992. Lithospheric thickness as a control on basalt geochemistry. Geology 20, 153–156.

49.   Elliott, T., & Spiegelman, M., 2003. Melt migration in oceanic crustal production: a U-series perspective. Treatise on geochemistry, 3, 659.

50.   Erdman, M.E., Lee, C.-T.A., Levander, A., Jiang, H., 2016. Role of arc magmatism and lower crustal foundering in controlling elevation history of the Nevadaplano and Colorado Plateau: A case study of pyroxenitic lower crust from central Arizona, USA. Earth and Planetary Science Letters 439, 48-57.

51.   Evans, K. A.,., 2012. The redox budget of subduction zones. Earth-Science Reviews 113(1–2), 11–32.

52.   Falloon, T.J., Danyushevsky, L.V., 2000. Melting of refractory mantle at 1.5, 2 and 2.5 GPa under anhydrous and H_2O-undersaturated conditions: Implications for the petrogenesis of high-Ca boninites and the influence of subduction components on mantle melting. Journal of Petrology 41, 257-283.

53.   Falloon, T.J., Green, D.H., Danyushevsky, L.V., McNeill, A.W., 2008. The composition of near-solidus partial melts of fertile peridotite at 1 and 1.5 GPa: implications for the petrogenesis of MORB. Journal of Petrology 49, 591-613.

54.   Farmer, G.L., Glazner, A.F., Kortemeier, W.T., Cosca, M.A., Jones, C.H., Moore, J.E., Schweickert, R.A., 2013. Mantle lithosphere as a source of post subduction magmatism, northern Sierra Nevada, California. Geosphere 9, 1102-1124.

55.   Förster, M.W., Prelević, D., Schmück, H.R., Buhre, S., Marschall, H.R., Mertz-Kraus, R., Jacob, D.E., 2018. Melting phlogopite-rich MARID: Lamproites and the role of alkalis in olivine-liquid Ni-partitioning. Chemical Geology 476, 429-440.

56.   Förster, M.W., Prelević, D., Schmück, H.R., Buhre, S., Veter, M., Mertz-Kraus, R., Foley, S.F., Jacob, D.E., 2017. Melting and dynamic metasomatism of mixed harzburgite+glimmerite mantle source: Implications for the genesis of orogenic potassic magmas. Chemical Geology 455, 182-191.

57.   Francis, D., 1986. The pyroxene paradox in MORB glasses—A signature of picritic parental magmas? Nature 319, 586-589.

58.   Gaetani, G.A., Grove, T.L., 1998. The influence of water on melting of mantle peridotite. Contributions to Mineralogy and Petrology 131, 323-346.

59.   Gaetani, G.A., O'Leary, J.A., Shimizu, N., Bucholz, C.E., Newville, M., 2012. Rapid reequilibration of H_2O and oxygen fugacity in olivine-hosted melt inclusions. Geology 40, 915-918.

60.   Gale, A., Langmuir, C. H., Dalton, C. A., 2014. The global systematics of ocean ridge basalts and their origin. Journal of Petrology 55(6), 1051-1082.

61.   Gale, A., Dalton, C.A., Langmuir, C.H., Su, Y., Schilling, J.G., 2013. The mean composition of ocean ridge basalts. Geochemistry, Geophysics, Geosystems 14, 489-518.

62.   Gao, S., Rudnick, R.L., Yuan, H.-L., Liu, X.-M., Liu, Y.-S., Xu, W.-L., Ling, W.-L., Ayers, J., Wang, X.-C., Wang, Q.-H., 2004. Recycling lower continental crust in the North China craton. Nature 432, 892.

63.   Gao, Y., Hoefs, J., Hellebrand, E., von der Handt, A., & Snow, J. E., 2007. Trace element zoning in pyroxenes from ODP Hole 735B gabbros: diffusive exchange or synkinematic crystal fractionation?. Contributions to Mineralogy and Petrology 153(4), 429-442.

64.   Gillis, K.M., Snow, J.E., Klaus, A., Abe, N., Adrião, Á.B., Akizawa, N., Ceuleneer, G., Cheadle, M.J., Faak, K., Falloon, T.J., 2014. Primitive layered gabbros from fast-spreading lower oceanic crust. Nature 505, 204-207.

65.   Green, D., Schmidt, M., Hibberson, W., 2004. Island-arc ankaramites: primitive melts from fluxed refractory lherzolitic mantle. Journal of Petrology 45, 391-403.

66.   Grocke S. B., Cottrell E., de Silva S., Kelley K. A., 2016. The role of crustal and eruptive processes versus source variations in controlling the oxidation state of iron in Central Andean magmas. Earth Planet. Sci. Lett. 440, 92–104.

67.   Grove, T.L., Chatterjee, N., Parman, S.W., Médard, E., 2006. The influence of H2O on mantle wedge melting. Earth and Planetary Science Letters 249, 74-89.

68.   Grove, T. L., D. C. Gerlach, and T. W. Sando, 1982. Origin of calc-alkaline series lavas at Medicine Lake volcano by fractionation, assimilation and mixing, Contributions to Mineralogy and Petrology 80(2), 160-182.

69.   Grove, T.L., Kinzler, R.J., Bryan, W.B., 1993. Fractionation of mid-ocean ridge basalt (MORB). Mantle flow and melt generation at mid-ocean ridges, 281-310.

70.   Hammouda, T., 2003. High-pressure melting of carbonated eclogite and experimental constraints on carbon recycling and storage in the mantle. Earth and Planetary Science Letters 214, 357-368.

71.   Helffrich, G.R., Wood, B.J., 2001. The Earth's mantle. Nature 412, 501-507.

72.   Hermann, J., Spandler, C.J., 2008. Sediment Melts at Sub-arc Depths: an Experimental Study. Journal of Petrology 49, 717-740.

73.   Herzberg, C., 2011. Identification of Source Lithology in the Hawaiian and Canary Islands: Implications for Origins. Journal of Petrology 52, 113-146.

74.   Herzberg, C., Asimow, P.D., 2015. PRIMELT3 MEGA.XLSM software for primary magma calculation: Peridotite primary magma MgO contents from the liquidus to the solidus. Geochemistry, Geophysics, Geosystems. doi: 10.1002/2014GC005631

75.   Herzberg, C., Asimow, P.D., Arndt, N., Niu, Y., Lesher, C.M., Fitton, J.G., Cheadle, M.J., Saunders, A.D., 2007. Temperatures in ambient mantle and plumes: Constraints from basalts, picrites, and komatiites. Geochem. Geophys. Geosyst. 8, Q02006-Q02006.

76.   Herzberg C. and Asimow P. D. (2008) Petrology of some oceanic island basalts: PRIMELT2.XLS software for primary magma calculation. Geochem. Geophys. Geosyst. 9.

77.   Herzberg, C., Gazel, E., 2009. Petrological evidence for secular cooling in mantle plumes. Nature 458, 619-622.

78.   Hildreth, W., Moorbath, S., 1988. Crustal contributions to arc magmatism in the Andes of Central Chile. Contributions to Mineralogy and Petrology 98, 455-489.

79.   Hirose, K., 1997. Melting experiments on lherzolite KLB-1 under hydrous conditions and generation of high-magnesian andesitic melts. Geology 25, 42-44.

80.   Hirose, K., Kawamoto, T., 1995. Hydrous partial melting of lherzolite at 1 GPa: The effect of H2O on the genesis of basaltic magmas. Earth and Planetary Science Letters 133, 463-473.

81.   Hirose, K., Kushiro, I., 1993. Partial melting of dry peridotites at high pressures: determination of compositions of melts segregated from peridotite using aggregates of diamond. Earth and Planetary Science Letters 114, 477-489.

82.   Hirschmann, M.M., 2000. Mantle solidus: Experimental constraints and the effects of peridotite composition. Geochem. Geophys. Geosyst. 1, 2000GC000070.

83.   Hirschmann M. M., Baker M. B., Stolper E. M., 1998. The Effect of Alkalis on the Silica Content of Mantle-Derived Melts. Geochim. Cosmochim. Acta 62, 883–902.

84.   Hirschmann, M.M., Kogiso, T., Baker, M.B., Stolper, E.M., 2003. Alkalic magmas generated by partial melting of garnet pyroxenite. Geology 31, 481-484.

85.   Hirschmann, M.M., Stolper, E.M., 1996. A possible role for garnet pyroxenite in the origin of the "garnet signature" in MORB. Contributions to Mineralogy and Petrology 124, 185-208.

86.   Hofmann, A.W., 1997. Mantle geochemistry: the message from oceanic volcanism. Nature 385, 219-229.

87.   Hofmann A. W., 2003. Sampling Mantle Heterogeneity through Oceanic Basalts: Isotopes and Trace Elements. Treatise Geochemistry Second Ed. 3, 67–101.

88.   Hofmann, A.W., White, W.W., 1982. Mantle plumes from ancient oceanic-crust. Earth Planet. Sci. Lett. 57, 421-421.

89.   Humayun, M., Qin, L.P., Norman, M.D., 2004. Geochemical evidence for excess iron in the mantle beneath Hawaii. Science 306, 91-94.

90.   Humphreys, M.C.S., Brooker, R.A., Fraser, D.G., Burgisser, A., Mangan, M.T., McCammon, C., 2015. Coupled Interactions between Volatile Activity and Fe Oxidation State during Arc Crustal Processes. Journal of Petrology 56, 795-814.

91.   Humphreys E. R. and Niu Y., 2009. On the composition of ocean island basalts (OIB): The effects of lithospheric thickness variation and mantle metasomatism. Lithos 112, 118–136.

92.   Ito, K., Kennedy, G.C., 1974. The composition of liquids formed by partial melting of eclogites at high temperatures and pressures. The Journal of Geology 82, 383-392.

93.   Jackson, M.G., Dasgupta, R., 2008. Compositions of HIMU, EM1, and EM2 from global trends between radiogenic isotopes and major elements in ocean island basalts. Earth and Planetary Science Letters 276, 175-186.

94.   Jackson M. G., Hart S. R., Koppers A. A. P., Staudigel H., Konter J., Blusztajn J., Kurz M. and Russell J. A., 2007. The return of subducted continental crust in Samoan lavas. Nature 448, 684–687.

95.   Jagoutz, O.E., 2010. Construction of the granitoid crust of an island arc. Part II: a quantitative petrogenetic model. Contributions to Mineralogy and Petrology 160, 359-381.

96.   Jenner, F.E., O'Neill, H.S.C., 2012. Analysis of 60 elements in 616 ocean floor basaltic glasses. Geochemistry, Geophysics, Geosystems 13, Q02005, DOI:10.1029/2011GC004009.

97.   Johnston, A.D., Wyllie, P.J., 1989. The system tonalite-peridotite-H2O at 30 kbar, with applications to hybridization in subduction zone magmatism. Contributions to Mineralogy and Petrology 102, 257-264.

98.   Kawamoto, T., Kanzaki, M., Mibe, K., Matsukage, K.N., Ono, S., 2012. Separation of supercritical slab-fluids to form aqueous fluid and melt components in subduction zone magmatism. Proceedings of the National Academy of Sciences 109, 18695-18700.

99.   Kelemen, P.B., 1995. Genesis of high Mg# andesites and the continental crust. Contributions to Mineralogy and Petrology 120, 1-19.

100.   Kelemen, P.B., Hart, S.R., Bernstein, S., 1998. Silica enrichment in the continental upper mantle via melt/rock reaction. Earth and Planetary Science Letters 164, 387-406.

101.   Kelemen P. B., Hirth G., Shimizu N., Spiegelman M. and Dick H. J.,1997. A review of melt migration processes in the adiabatically upwelling mantle beneath oceanic spreading ridges. Philos. Trans. R. Soc. London. Ser. A Math. Phys. Eng. Sci. 355, 283–318.

102.   Kelemen, P.B., Whitehead, J.A., Aharonov, E., Jordahl, K.A., 1995. Experiments on flow focusing in soluble porous media, with applications to melt extraction from the mantle. Journal of Geophysical Research: Solid Earth 100, 475-496.

103.   Kelley, K.A., Cottrell, E., 2009. Water and the Oxidation State of Subduction Zone Magmas. Science 325, 605-607.

104.   Kepezhinskas, P., M. J. Defant, and M. S. Drummond., 1996. Progressive enrichment of island arc mantle by melt-peridotite interaction inferred from Kamchatka xenoliths, Geochimica et Cosmochimica Acta 60(7), 1217-1229, doi:10.1016/0016-7037(96)00001-4.

105.   Keshav, S., Gudfinnsson, G.H., Sen, G., Fei, Y., 2004. High-pressure melting experiments on garnet clinopyroxenite and the alkalic to tholeiitic transition in ocean-island basalts. Earth and Planetary Science Letters 223, 365-379.

106.   Kessel R., Ulmer P., Pettke T., Schmidt M. W. and Thompson A. B. (2004) A novel approach to determine high-pressure high-temperature fluid and melt compositions using diamond-trap experiments. Am. Mineral. 89, 1078–1086.

107.   Kiseeva, E.S., Litasov, K.D., Yaxley, G.M., Ohtani, E., Kamenetsky, V.S., 2013. Melting and Phase Relations of Carbonated Eclogite at 9–21 GPa and the Petrogenesis of Alkali-Rich Melts in the Deep Mantle. Journal of Petrology 54(8), 1555-1583.

108.   Klein, E.M., Langmuir, C.H., 1987. Global correlations of ocean ridge basalt chemistry with axial depth and crustal thickness. J. Geophys. Res. 92, 8089-8089.

109.   Kogiso, T., Hirose, K., Takahashi, E., 1998. Melting experiments on homogeneous mixtures of peridotite and basalt: application to the genesis of ocean island basalts. Earth and Planetary Science Letters 162, 45-61.

110.   Kogiso, T., Hirschmann, M.M., 2001. Experimental study of clinopyroxenite partial melting and the origin of ultra-calcic melt inclusions. Contributions to Mineralogy and Petrology 142, 347-360.

111.   Kogiso, T., Hirschmann, M.M., 2006. Partial melting experiments of bimineralic eclogite and the role of recycled mafic oceanic crust in the genesis of ocean island basalts. Earth and Planetary Science Letters 249, 188-199.

112.   Kogiso, T., Hirschmann, M.M., Frost, D.J., 2003. High-pressure partial melting of garnet pyroxenite: possible mafic lithologies in the source of ocean island basalts. Earth and Planetary Science Letters 216, 603-617.

113.   Kogiso, T., Hirschmann, M.M., Pertermann, M., 2004. High-pressure Partial Melting of Mafic Lithologies in the Mantle. Journal of Petrology 45, 2407-2422.

114.   Kornprobst, J., 1970. Les péridotites et les pyroxénolites du massif ultrabasique de Beni Bouchera: une étude expérimentale entre 1100 et 1550°C, sous 15 à 30 kilobars de pression sèche. Contributions to Mineralogy and Petrology 29, 290-309

115.   Kushiro, I., 1996. Partial melting of fertile mantle peridotite at high pressures: an experimental study using aggregates of diamond. Geophysical Monograph, American Geophysical Union 95, 109-122.

116.   Lackey, J.S., Valley, J.W., Saleeby, J.B., 2005. Supracrustal input to magmas in the deep crust of Sierra Nevada batholith: Evidence from high-δ^{18}O zircon. Earth and Planetary Science Letters 235, 315-330.

117.   Lambart, S., 2017. No direct contribution of recycled crust in Icelandic basalts. Geochemical Perspectives Letters, 4. doi: 10.7185/geochemlet.1728

118.   Lambart, S., Koornneef, J. M., Millet, M. A., Davies, G. R., Cook, M., Lissenberg, C. J., 2019. Highly heterogeneous depleted mantle recorded in the lower oceanic crust. Nature Geoscience 12(6), 482. doi: 10.1038/s41561-019-0368-9

119.   Lambart, S., Baker, M.B., Stolper, E.M., 2016. The role of pyroxenite in basalt genesis: Melt-PX, a melting parameterization for mantle pyroxenites between 0.9 and 5 GPa. Journal of Geophysical Research: Solid Earth, 121(8), 5708-5735.

120.   Lambart, S., Laporte, D., Provost, A., Schiano, P., 2012. Fate of Pyroxenite-derived Melts in the Peridotitic Mantle: Thermodynamic and Experimental Constraints. Journal of Petrology 53, 451-476.

121.   Lambart, S., Laporte, D., Schiano, P., 2009. An experimental study of pyroxenite partial melts at 1 and 1.5 GPa: Implications for the major-element composition of Mid-Ocean Ridge Basalts. Earth and Planetary Science Letters 288, 335-347.

122.   Lambart, S., Laporte, D., Schiano, P., 2013. Markers of the pyroxenite contribution in the major-element compositions of oceanic basalts: Review of the experimental constraints. Lithos 160-161, 14-36.

123.   Langmuir, C.H., 1989. Geochemical consequences of in situ crystallization. Nature 340, 199.

124.   Langmuir, C.H., Klein, E.M., Plank, T., 1992. Petrological Systematics of Mid-Ocean Ridge Basalts: Constraints on Melt Generation Beneath Ocean Ridges. Geophysical Monograph - American Geophysical Union. 71, 183-280.

125.   Laporte D., Toplis M. J., Seyler M., Devidal J. L., 2004. A new experimental technique for extracting liquids from peridotite at very low degrees of melting: Application to partial melting of depleted peridotite. Contributions to Mineralogy and Petrology 146, 463–484.

126.   Le Bas M. J. , Maitre R. W. L., Streckeisen A., Zanettin B., 1986. A chemical classification of volcanic rocks based on the total alkali-silica diagram. Journal of Petrology 27, 745–750.

127.   Le Maitre, R.W., Streckeisen, A., Zanettin, B., Le Bas, M., Bonin, B., Bateman, P., 2005. Igneous rocks: a classification and glossary of terms: recommendations of the International Union of Geological Sciences Subcommission on the Systematics of Igneous Rocks. Cambridge University Press.

128.   Le Roux, V., Dasgupta, R., Lee, C.T.A., 2011. Mineralogical heterogeneities in the Earth's mantle: Constraints from Mn, Co, Ni and Zn partitioning during partial melting. Earth and Planetary Science Letters 307, 395-408.

129.   Le Roux, V., Lee, C.-T., Turner, S., 2010. Zn/Fe systematics in mafic and ultramafic systems: Implications for detecting major element heterogeneities in the Earth's mantle. Geochimica et Cosmochimica Acta 74, 2779-2796.

130.   Lee, C.-T.A., Cheng, X., Horodyskyj, U., 2006. The development and refinement of continental arcs by primary basaltic magmatism, garnet pyroxenite accumulation, basaltic recharge and delamination: insights from the Sierra Nevada. Contributions to Mineralogy and Petrology 151, 222-242.

131.   Lee, C.-T.A., Leeman, W.P., Canil, D., A, L.Z.-X., 2005. Similar V/Sc Systematics in MORB and Arc Basalts: Implications for the Oxygen Fugacities of their Mantle Source Regions. Journal of Petrology 46, 2313-2336.

132.   Lee, C.-T.A., Luffi, P., Le Roux, V., Dasgupta, R., Albaréde, F., Leeman, W.P., 2010. The redox state of arc mantle using Zn/Fe systematics. Nature 468, 681-685.

133.   Lee C. T. A., Luffi P., Plank T., Dalton H., Leeman W. P., 2009. Constraints on the depths and temperatures of basaltic magma generation on Earth and other terrestrial planets using new thermobarometers for mafic magmas. Earth Planet. Sci. Lett. 279, 20–33.

134.   Lissenberg, C.J., Dick, H.J., 2008. Melt–rock reaction in the lower oceanic crust and its implications for the genesis of mid-ocean ridge basalt. Earth and Planetary Science Letters 271, 311-325.

135.   Lissenberg, C.J., MacLeod, C.J., 2016. A Reactive Porous Flow Control on Mid-ocean Ridge Magmatic Evolution. Journal of Petrology 57, 2195-2220.

136.   Lissenberg, C. J., MacLeod, C. J., Bennett, E. N., 2019. Consequences of a crystal mush-dominated magma plumbing system: a mid-ocean ridge perspective. Philosophical Transactions of the Royal Society A, 377(2139), 20180014.

137.	Lissenberg, C.J., MacLeod, C.J., Howard, K.A., Godard, M., 2013. Pervasive reactive melt migration through fast-spreading lower oceanic crust (Hess Deep, equatorial Pacific Ocean). Earth and Planetary Science Letters 361, 436-447.

138.	Lustrino, M., 2005. How the delamination and detachment of lower crust can influence basaltic magmatism. Earth-Science Reviews 72, 21-38.

139.	Mallik, A., Dasgupta, R., 2012. Reaction between MORB-eclogite derived melts and fertile peridotite and generation of ocean island basalts. Earth and Planetary Science Letters 329, 97-108.

140.	Mallik, A., Dasgupta, R., 2013. Reactive Infiltration of MORB-Eclogite-Derived Carbonated Silicate Melt into Fertile Peridotite at 3 GPa and Genesis of Alkalic Magmas. Journal of Petrology 54, 2267-2300.

141.	Mallik, A., Dasgupta, R., 2014. Effect of variable CO_2 on eclogite-derived andesite and lherzolite reaction at 3 GPa: Implications for mantle source characteristics of alkalic ocean island basalts. Geochemistry, Geophysics, Geosystems 15, 1533-1557.

142.	Mallik, A., Dasgupta, R., Tsuno, K., Nelson, J., 2016. Effects of water, depth and temperature on partial melting of mantle-wedge fluxed by hydrous sediment-melt in subduction zones. Geochimica et Cosmochimica Acta 195, 226-243.

143.	Mallik, A., Nelson, J., Dasgupta, R., 2015. Partial melting of fertile peridotite fluxed by hydrous rhyolitic melt at 2–3 GPa: implications for mantle wedge hybridization by sediment melt and generation of ultrapotassic magmas in convergent margins. Contributions to Mineralogy and Petrology 169, 1-24.

144.	Mallik, A., Li, Y., & Wiedenbeck, M., 2018. Nitrogen evolution within the Earth's atmosphere–mantle system assessed by recycling in subduction zones. Earth and Planetary Science Letters 482, 556–566.

145.	Marschall, H.R., Schumacher, J.C., 2012. Arc magmas sourced from melange diapirs in subduction zones. Nature Geoscience 5, 862-867.

146.	Matzen, A.K., Baker, M.B., Beckett, J.R., Stolper, E.M., 2013. The Temperature and Pressure Dependence of Nickel Partitioning between Olivine and Silicate Melt. Journal of Petrology 54(12), 2521-2545.

147.	Matzen, A.K., Baker, M.B., Beckett, J.R., Wood, B.J., Stolper, E.M., 2017a. The effect of liquid composition on the partitioning of Ni between olivine and silicate melt. Contributions to Mineralogy and Petrology172, 3-3, doi: 10.1007/s00410-016-1319-8.

148.	Matzen, A. K., Wood, B. J., Baker, M. B., & Stolper, E. M., 2017b. The roles of pyroxenite and peridotite in the mantle sources of oceanic basalts. Nature Geoscience, 10(7), 530.

149.	McBirney, A.R., Noyes, R.M., 1979. Crystallization and layering of the Skaergaard intrusion. Journal of Petrology 20, 487-554.

150.	McKenzie D., Jackson J., Priestley K., 2005 Thermal structure of oceanic and continental lithosphere. Earth and Planetary Science Letters 233, 337–349.

151.   Médard, E., Schmidt, M.W., Schiano, P., Ottolini, L., 2005. Melting of amphibole-bearing wehrlites: an experimental study on the origin of ultra-calcic nepheline-normative melts. Journal of Petrology 47, 481-504.

152.   Mibe, K., Kanzaki, M., Kawamoto, T., Matsukage, K.N., Fei, Y., Ono, S., 2007. Second critical endpoint in the peridotite-H2O system. Journal of Geophysical Research: Solid Earth 112.

153.   Mibe, K., Kawamoto, T., Matsukage, K.N., Fei, Y., Ono, S., 2011. Slab melting versus slab dehydration in subduction-zone magmatism. Proceedings of the National Academy of Sciences of the United States of America 108, 8177-8182.

154.   Natland, J.H., Dick, H.J., 1996. Melt migration through high-level gabbroic cumulates of the East Pacific Rise at Hess Deep: the origin of magma lenses and the deep crustal structure of fast-spreading ridges, Proceedings-Ocean Drilling Program Scientific Results. National Science Foundation, pp. 21-58.

155.   Navon, O., Stolper, E., 1987. Geochemical consequences of melt percolation: the upper mantle as a chromatographic column. The Journal of Geology 285-307.

156.   Neave, D. A., Namur, O., Shorttle, O., Holtz, F., 2019. Magmatic evolution biases basaltic records of mantle chemistry towards melts from recycled sources. Earth and Planetary Science Letters, 520, 199–211. doi:10.1016/j.epsl.2019.06.003

157.   Nelson, W.R., Dorais, M.J., Christiansen, E.H., Hart, G.L., 2013. Petrogenesis of Sierra Nevada plutons inferred from the Sr, Nd, and O isotopic signatures of mafic igneous complexes in Yosemite Valley, California. Contributions to Mineralogy and Petrology 165, 397-417.

158.   .,.Ni, H., Zhang, L., Xiong, X., Mao, Z., Wang, J., 2017. Supercritical fluids at subduction zones: Evidence, formation condition, and physicochemical properties. Earth-Science Reviews 167, 62-71.

159.   Nielsen, S.G., Marschall, H.R., 2017. Geochemical evidence for mélange melting in global arcs. Science Advances 3.

160.   Niu Y., Wilson M., Humphreys E. R. and O'Hara M. J., 2011. The origin of intra-plate ocean island basalts (OIB): The lid effect and its geodynamic implications. Journal of Petrology 52, 1443–1468.

161.   Niu, Y., O'Hara, M. J., 2008. Global correlations of ocean ridge basalt chemistry with axial depth: a new perspective. Journal of Petrology, 49(4), 633-664.

162.   O'Hara, M., 1965. Primary magmas and the origin of basalts. Scottish Journal of Geology 1, 19-40.

163.   O'Hara, M., 1977. Geochemical evolution during fractional crystallisation of a periodically refilled magma chamber. Nature 266, 503.

164.   O'Hara, M., 1976. Data reduction and projection schemes for complex compositions. Third progress report of research supported by NERC in Edinburgh and Manchester Universities (1972-75) 6, 103-126.

165.   O'Neill, H.S.C., Jenner, F.E., 2012. The global pattern of trace-element distributions in ocean floor basalts. Nature 491, 698.

166.   Otamendi, J.E., Ducea, M.N., Bergantz, G.W., 2012. Geological, petrological and geochemical evidence for progressive construction of an arc crustal section, Sierra de Valle Fertil, Famatinian Arc, Argentina. Journal of Petrology 53, 761-800.

167.   Patiño Douce, A. E., 1999. What do experiments tell us about the relative contributions of crust and mantle to the origin of granitic magmas?, Geological Society, London, Special Publications 168(1), 55-75, doi:10.1144/gsl.sp.1999.168.01.05.

168.   Pertermann, M., Hirschmann, M.M., 2003a. Partial melting experiments on a MORB-like pyroxenite between 2 and 3 GPa: Constraints on the presence of pyroxenite in basalt source regions from solidus location and melting rate. J. Geophys. Res. Solid Earth 108, 2125-2125.

169.   Pertermann, M., Hirschmann, M.M., 2003b. Anhydrous partial melting experiments on a MORB-like eclogite: phase relations, phase compositions and mineral-melt partitioning of major elements at 2-3 GPa. Journal of Petrology 44, 2173-2201.

170.   Pertermann, M., Hirschmann, M. M., Hametner, K., Günther, D., Schmidt, M. W., 2004. Experimental determination of trace element partitioning between garnet and silica-rich liquid during anhydrous partial melting of MORB-like eclogite. Geochemistry, Geophys. Geosystems 5, 5.

171.   Phipps Morgan J., 2001. Thermodynamics of pressure release melting of a veined plum pudding mantle. Geochemistry, Geophys. Geosystems 2, 2000GC000049.

172.   Pickering-Witter, J., Johnston, A.D., 2000. The effects of variable bulk composition on the melting systematics of fertile peridotitic assemblages. Contributions to Mineralogy and Petrology 140, 190-211.

173.   Pilet, S., Baker, M.B., Stolper, E.M., 2008. Metasomatized Lithosphere and the Origin of Alkaline Lavas. Science 320, 916-919.

174.   Pirard, C., Hermann, J., 2014. Experimentally determined stability of alkali amphibole in metasomatised dunite at sub-arc pressures. Contributions to Mineralogy and Petrology 169, 1-26.

175.   Pirard, C., Hermann, J., 2015. Focused fluid transfer through the mantle above subduction zones. Geology 43, 915-918.

176.   Plank, T., 2005. Constraints from Thorium/Lanthanum on Sediment Recycling at Subduction Zones and the Evolution of the Continents. Journal of Petrology 46, 921-944.

177.   Poli, S., Schmidt, M.W., 1995. H2O transport and release in subduction zones: Experimental constraints on basaltic and andesitic systems. Journal of Geophysical Research: Solid Earth 100, 22299-22314.

178.   Prouteau, G., Scaillet, B., Pichavant, M., Maury, R., 2001. Evidence for mantle metasomatism by hydrous silicic melts derived from subducted oceanic crust. Nature 410, 197-200.

179.   Prytulak, J., Elliott, T., 2007. TiO2 enrichment in ocean island basalts. Earth and Planetary Science Letters 263, 388-403.

180.   Putirka K. D., 2008. Thermometers and barometers for volcanic systems. Rev. Mineral. Geochemistry 69, 61–120.

181.   Qin, L., Humayun, M., 2008. The Fe/Mn ratio in MORB and OIB determined by ICP-MS. Geochimica et Cosmochimica Acta 72, 1660-1677.

182.   Rampone, E., Hofmann, A.W., 2012. A global overview of isotopic heterogeneities in the oceanic mantle. Lithos 148, 247-261.

183.   Rapp, R., Shimizu, N., Norman, M., Applegate, G., 1999. Reaction between slab-derived melts and peridotite in the mantle wedge: experimental constraints at 3.8 GPa. Chemical Geology 160, 335-356.

184.   Rosenthal, A., Yaxley, G.M., Crichton, W.A., Kovacs, I., Spandler, C., Hermann, J., Sándorné, J.K., Rose-Koga, E., Pelleter, A.-A., 2018. Phase relations and melting of nominally 'dry'residual eclogites with variable CaO/Na2O from 3 to 5 GPa and 1250 to 1500° C; implications for refertilisation of upwelling heterogeneous mantle. Lithos 314, 506-519.

185.   Rosenthal, A., Yaxley, G.M., Green, D.H., Hermann, J., Kovacs, I., Spandler, C., 2014. Continuous eclogite melting and variable refertilisation in upwelling heterogeneous mantle. Sci. Rep. 4, 6099.

186.   Sadofsky, S.J., Portnyagin, M., Hoernle, K., van den Bogaard, P., 2008. Subduction cycling of volatiles and trace elements through the Central American volcanic arc: evidence from melt inclusions. Contributions to Mineralogy and Petrology 155, 433-456.

187.   Salters, V.J.M., Dick, H.J.B., 2002. Mineralogy of the mid-ocean-ridge basalt source from neodymium isotopic composition of abyssal peridotites. Nature 418, 68-72.

188.   Schiano, P., Birck, J.-L., Allègre, C.J., 1997. Osmium-strontium-neodymium-lead isotopic covariations in mid-ocean ridge basalt glasses and the heterogeneity of the upper mantle. Earth and Planetary Science Letters 150, 363-379.

189.   Schiano, P., Eiler, J.M., Hutcheon, I.D., Stolper, E.M., 2000. Primitive CaO-rich, silica-undersaturated melts in island arcs: Evidence for the involvement of clinopyroxene-rich lithologies in the petrogenesis of arc magmas. Geochemistry, Geophysics, Geosystems 1, 1018, doi:10.1029/1999GC000032.

190.   Schwab, B.E., Johnston, A.D., 2001. Melting Systematics of Modally Variable, Compositionally Intermediate Peridotites and the Effects of Mineral Fertility. Journal of Petrology 42, 1789-1811.

191.   Sekine, T., Wyllie, P.J., 1982. Phase relationships in the system KAlSiO4-Mg2SiO4-SiO2-H2O as a model for hybridization between hydrous siliceous melts and peridotite. Contributions to Mineralogy and Petrology 79, 368-374.

192.   ., .Shen, A.H., Keppler, H., 1997. Direct observation of complete miscibility in the albite–H2O system. Nature 385, 710-710.

193.   Shorttle, O., 2015. Geochemical variability in MORB controlled by concurrent mixing and crystallisation. Earth and Planetary Science Letters, 424, 1-14.

194.   Skora, S., Blundy, J., 2010. High-pressure Hydrous Phase Relations of Radiolarian Clay and Implications for the Involvement of Subducted Sediment in Arc Magmatism. Journal of Petrology 51, 2211-2243.

195.   Sleep, N.H., 1990. Hotspots and mantle plumes: Some phenomenology. Journal of Geophysical Research: Solid Earth 95, 6715-6736.

196.   Sobolev, A.V., Hofmann, A.W., Kuzmin, D.V., Yaxley, G., Arndt, N., Chung, S.L., Danyushevsky, L.V., Elliott, T., Frey, F.A., Garcia, M.O. and Gurenko, A.A., 2007. The amount of recycled crust in sources of mantle-derived melts. Science 316, 412-412.

197.   Sobolev, A.V., Hofmann, A.W., Sobolev, S.V., Nikogosian, I.K., 2005. An olivine-free mantle source of Hawaiian shield basalts. Nature 434, 590-597.

198.   Spandler, C., Yaxley, G., Green, D., Scott, D., 2010. Experimental phase and melting relations of metapelite in the upper mantle: implications for the petrogenesis of intraplate magmas. Contributions to Mineralogy and Petrology 160, 569-589.

199.   Spandler, C., Yaxley, G., Green, D.H., Rosenthal, A., 2008. Phase Relations and Melting of Anhydrous K-bearing Eclogite from 1200 to 1600°C and 3 to 5 GPa. J. Petrology 49, 771-795.

200.   Syracuse, E.M., van Keken, P.E., Abers, G.A., 2010. The global range of subduction zone thermal models. Physics of the Earth and Planetary Interiors 183, 73-90.

201.   Takahashi E., 1986. Melting of a dry peridotite KLB-1 up to 14 GPa: Implications on the Origin of peridotitic upper mantle. J. Geophys. Res. 91, 9367.

202.   Tamura, Y., Ishizuka, O., Stern, R.J., Nichols, A.R.L., Kawabata, H., Hirahara, Y., Chang, Q., Miyazaki, T., Kimura, J.-I., Embley, R.W., Tatsumi, Y., 2014. Mission Immiscible: Distinct Subduction Components Generate Two Primary Magmas at Pagan Volcano, Mariana Arc. Journal of Petrology 55, 63-101.

203.   Tang, M., Erdman, M., Eldridge, G., Lee, C.-T.A., 2018. The redox "filter" beneath magmatic orogens and the formation of continental crust. Science Advances 4.

204.   Tang, M., Lee, C.-T.A., Chen, K., Erdman, M., Costin, G., Jiang, H., 2019. Nb/Ta systematics in arc magma differentiation and the role of arclogites in continent formation. Nature Communications 10, 235.

205.   Tatsumi, Y., 2001. Geochemical modeling of partial melting of subducting sediments and subsequent melt-mantle interaction: Generation of high-Mg andesites in the Setouchi volcanic belt, southwest Japan. Geology 29, 323-326.

206.   Tatsumi, Y., Kogiso, T., 2003. The subduction factory: its role in the evolution of the Earth's crust and mantle. Geological Society, London, Special Publications 219, 55 LP-80.

207.   Tatsumi, Y., Sakuyama, M., Fukuyama, H., Kushiro, I., 1983. Generation of Arc Basalt Magmas and Thermal Structure of the Mantle Wedge in Subduction Zones. J. Geophys. Res. 88, 5815-5825.

208.   Tenner, T.J., Hirschmann, M.M., Humayun, M., 2012. The effect of H2O on partial melting of garnet peridotite at 3.5 GPa. Geochem. Geophys. Geosyst. 13, Q03016-Q03016.

209.   Thompson, R.N., 1974. Primary Basalts and Magma Genesis I. Skye, North-West Scotland. Contributions to Mineralogy and Petrology 45, 317-341.

210.   Thompson, R. N., 1975. Primary basalts and magma genesis. Contributions to Mineralogy and Petrology 52(3), 213-232.

211.   Thomson, A.R., Walter, M.J., Kohn, S.C., Brooker, R.A., 2016. Slab melting as a barrier to deep carbon subduction. Nature 529, 76-79.

212.   Till, C.B., Grove, T.L., Withers, A.C., 2012. The beginnings of hydrous mantle wedge melting. Contributions to Mineralogy and Petrology 163, 669-688.

213.   Tollan P. and Hermann J., 2019. Arc magmas oxidized by water dissociation and hydrogen incorporation in orthopyroxene. Nature Geoscience 12, 667–671.

214.   Tsuruta, K., Takahashi, E., 1998. Melting study of an alkali basalt JB-1 up to 12.5 GPa: behavior of potassium in the deep mantle. Physics of the Earth and Planetary Interiors 107, 119-130.

215.   Tuff, J., Takahashi, E., Gibson, S., 2005. Experimental constraints on the role of garnet pyroxenite in the genesis of high-Fe mantle plume derived melts. Journal of Petrology 46, 2023-2058.

216.   Turner, S.J., Langmuir, C.H., 2015. The global chemical systematics of arc front stratovolcanoes: Evaluating the role of crustal processes. Earth and Planetary Science Letters 422, 182-193.

217.   Turner, S.J., Langmuir, C.H., Katz, R.F., Dungan, M.A., Escrig, S., 2016. Parental arc magma compositions dominantly controlled by mantle-wedge thermal structure. Nature Geosci 9, 772-776.

218.   Walker Jr, B.A., Bergantz, G.W., Otamendi, J.E., Ducea, M.N., Cristofolini, E.A., 2015. A MASH zone revealed: the mafic complex of the Sierra Valle Fértil. Journal of Petrology 56, 1863-1896.

219.   Walter, M.J., 1998. Melting of Garnet Peridotite and the Origin of Komatiite and Depleted Lithosphere. J. Petrology 39, 29-60.

220.   Wang, Y., Foley, S.F., 2018. Hybridization Melting Between Continent-Derived Sediment and Depleted Peridotite in Subduction Zones. Journal of Geophysical Research: Solid Earth 123, 3414-3429.

221.   Wang, Y., Prelević, D., Buhre, S., Foley, S.F., 2017. Constraints on the sources of post-collisional K-rich magmatism: The roles of continental clastic sediments and terrigenous blueschists. Chemical Geology 455, 192-207.

222.   Wang, Z., Gaetani, G.A., 2008. Partitioning of Ni between olivine and siliceous eclogite partial melt: experimental constraints on the mantle source of Hawaiian basalts. Contributions to Mineralogy and Petrology 156, 661-678.

223.   Wasylenki, L.E., Baker, M.B., Kent, A.J.R., Stolper, E.M., 2003. Near-solidus Melting of the Shallow Upper Mantle: Partial Melting Experiments on Depleted Peridotite. Journal of Petrology 44, 1163-1191.

224.   Weatherley, S.M., Katz, R.F., 2012. Melting and channelized magmatic flow in chemically heterogeneous, upwelling mantle. Geochemistry, Geophysics, Geosystems 13.

225.   Weatherley, S.M., Katz, R.F., 2016. Melt transport rates in heterogeneous mantle beneath mid-ocean ridges. Geochimica et Cosmochimica Acta 172, 39-54.

226.   White, W., Klein, E., 2014. Composition of the Oceanic Crust. Treatise on Geochemistry (Second Edition),. 4, 457-496. doi: 10.1016/B978-0-08-095975-7.00315-6.

227.   Woodhead, J.D., Hergt, J.M., Davidson, J.P., Eggins, S.M., 2001. Hafnium isotope evidence for 'conservative' element mobility during subduction zone processes. Earth and Planetary Science Letters 192, 331-346.

228.   Yang, Z. F., Li, J., Jiang, Q. B., Xu, F., Guo, S. Y., Li, Y., Zhang, J., 2019. Using major element logratios to recognize compositional patterns of basalt: implications for source lithological and compositional heterogeneities. Journal of Geophysical Research: Solid Earth. doi: 10.1029/2018JB016145

229.   Yang, Z. F., Li, J., Liang, W. F., Luo, Z. H., 2016. On the chemical markers of pyroxenite contributions in continental basalts in Eastern China: implications for source lithology and the origin of basalts. Earth-science reviews, 157, 18-31.

230.   Yang, Z. F., Zhou, J. H., 2013. Can we identify source lithology of basalt? Scientific Reports, 3, 1856.

231.   Yasuda, A., Fujii, T., Kurita, K., 1994. Melting phase relations of an anhydrous mid-ocean ridge basalt from 3 to 20 GPa: Implications for the behavior of subducted oceanic crust in the mantle. J. Geophys. Res. 99, 9401-9414.

232.   Yaxley, G., Brey, G., 2004. Phase relations of carbonate-bearing eclogite assemblages from 2.5 to 5.5 GPa: implications for petrogenesis of carbonatites. Contributions to Mineralogy and Petrology 146, 606-619.

233.   Yaxley, G., Sobolev, A.V., 2007. High-pressure partial melting of gabbro and its role in the Hawaiian magma source. Contributions to Mineralogy and Petrology 154, 371-383.

234.   Yaxley, G.M., Green, D.H., 1998. Reactions between eclogite and peridotite: mantle refertilisation by subduction of oceanic crust. Schweiz. Mineral. Petrogr. Mitt 78, 243-255.

235.   Zhang, G.L., Sun, W.D., Seward, G., 2018. Mantle source and magmatic evolution of the dying spreading ridge in the South China Sea. Geochemistry, Geophysics, Geosystems 19, 4385-4399.

236.   Zindler A., Staudigel H. and Batiza R., 1984. Isotope and trace element geochemistry of young Pacific seamounts: implications for the scale of upper mantle heterogeneity. Earth Planet. Sci. Lett. 70, 175–195.